Electrochemical Energy Reviews (2022) 5: 2
https://doi.org/10.1007/s41918-022-00134-w

REVIEW ARTICLE

Lead-Carbon Batteries toward Future Energy Storage: From Mechanism and Materials to Applications

Jian Yin[1,4] · Haibo Lin[1,3] · Jun Shi[1,3] · Zheqi Lin[1] · Jinpeng Bao[1] · Yue Wang[1] · Xuliang Lin[2] · Yanlin Qin[2] · Xueqing Qiu[2,5] · Wenli Zhang[1,2,4]

Received: 17 December 2020 / Revised: 2 June 2021 / Accepted: 26 September 2021 / Published online: 27 July 2022
© The Author(s) 2022

Abstract

The lead acid battery has been a dominant device in large-scale energy storage systems since its invention in 1859. It has been the most successful commercialized aqueous electrochemical energy storage system ever since. In addition, this type of battery has witnessed the emergence and development of modern electricity-powered society. Nevertheless, lead acid batteries have technologically evolved since their invention. Over the past two decades, engineers and scientists have been exploring the applications of lead acid batteries in emerging devices such as hybrid electric vehicles and renewable energy storage; these applications necessitate operation under partial state of charge. Considerable endeavors have been devoted to the development of advanced carbon-enhanced lead acid battery (i.e., lead-carbon battery) technologies. Achievements have been made in developing advanced lead-carbon negative electrodes. Additionally, there has been significant progress in developing commercially available lead-carbon battery products. Therefore, exploring a durable, long-life, corrosion-resistive lead dioxide positive electrode is of significance. In this review, the possible design strategies for advanced maintenance-free lead-carbon batteries and new rechargeable battery configurations based on lead acid battery technology are critically reviewed. Moreover, a synopsis of the lead-carbon battery is provided from the mechanism, additive manufacturing, electrode fabrication, and full cell evaluation to practical applications.

Keywords Lead acid battery · Lead-carbon battery · Partial state of charge · PbO_2 · Pb

1 Introduction

Sustainable, low-cost, and green energy is a prerequisite for the advanced productivity of modern society [1, 2]. Currently, human society is facing the exhaustion of fossil fuels and the pollution caused by the burning of fossil fuels. Energy-saving technologies and advanced

We commemorate the "giant" of lead acid battery technology, an academician of the Bulgarian Academy of Sciences, Professor Dr. Detchko Pavlov (1930–2017).

✉ Haibo Lin
lhb910@jlu.edu.cn

✉ Xueqing Qiu
cexqqiu@scut.edu.cn

✉ Wenli Zhang
wlzhang@gdut.edu.cn

[1] State Key Laboratory of Inorganic Synthesis and Preparative Chemistry, College of Chemistry, Jilin University, 2699 Qianjin Street, Chaoyang District, Changchun 130012, Jilin, China

[2] Guangdong Provincial Key Laboratory of Plant Resources Biorefinery, School of Chemical Engineering and Light Industry, Guangdong University of Technology (GDUT), 100 Waihuan Xi Road, Panyu District, Guangzhou 510006, Guangdong, China

[3] School of Chemical Engineering and New Energy Materials, Zhuhai College of Science and Technology, Zhuhai 519041, Guangdong, China

[4] Materials Science and Engineering, Physical Science and Engineering Division, King Abdullah University of Science and Technology (KAUST), Thuwal 23955-6900, Saudi Arabia

[5] School of Chemistry and Chemical Engineering, South China University of Technology (SCUT), Guangzhou 510640, Guangdong, China

technologies for converting renewable energy into electricity are changing the world. Hybrid electric vehicles (HEVs) and electricity generation from renewable energy could reduce our dependence on fossil fuels [3, 4]. In an HEV, the battery module can provide an energy pulse to start the internal combustion engine (ICE) and harvest braking energy in the stop process, which dramatically enhances the energy efficiency of the ICE. The generation of electricity from renewable energy is intermittent and transient, which necessitates electrochemical energy storage devices to smooth its electricity input to an electrical grid [5]. Therefore, it is crucial to develop low-cost, green, and high-efficiency energy storage devices for the development of HEVs and the storage of electricity generated from renewable energy [6].

Despite the wide application of high-energy-density lithium-ion batteries (LIBs) in portable devices, electric vehicles, and emerging large-scale energy storage applications, lead acid batteries (LABs) have been the most common electrochemical power sources for medium to large energy storage systems since their invention by Gaston Planté in 1859 [7, 8]. In 2018, LABs occupied 70% of the world's rechargeable battery market, with a revenue of 80 billion USD and a total production of 600 GWh [9]. In particular, LABs are indispensable in stationary storage in that stationary energy storage is less sensitive to the lower energy density of LABs (35–40 Wh kg^{-1}) than LIBs (> 200 Wh kg^{-1}). In addition, LABs are very inexpensive rechargeable batteries in terms of the cost per unit energy volume (150 USD kWh^{-1}) [10]. Although Pb is toxic, their sealed maintenance-free design and numerous mature recycling technologies have made LABs "green" batteries [11]. Benefitting from its mature manufacturing process, lack of need for maintenance, high safety level, and reliable performance, this type of battery has been used in a wide range of applications in the start, light, and ignition (SLI) of automobiles [12], telecommunication [13], uninterruptable power supply (UPS) [14], remote area power supply (RAPS) [15], and low-speed electric vehicles [16, 17]. In this section, the history of the LAB is elucidated first, followed by an introduction to its challenges and opportunities in the twenty-first century.

1.1 Invention and a Brief History of Lead Acid Batteries (LABs)

A brief history of LABs is presented in Fig. 1. The detailed stories and technological advancements of LABs during the past three centuries can be found in Table 1 and the relevant literature [18]. The evolution of LABs can be divided into three stages: their invention in the nineteenth century, scientific and technical advancement in the twentieth century, and advanced design and scientific development in the twenty-first century (plotted in three colors in Fig. 1). Prior to the invention of LABs, scientists empirically designed or invented batteries, such as Volta cells and Daniel cells. LABs were first invented by a French physicist named Gaston Planté in 1859, ten years before the invention of a mechanical electricity generator by Michael Faraday [7]. A Planté cell is essentially prepared by immersing two lead plates in sulfuric acid and then can be charged and discharged repeatedly. Due to the anodic oxidation of the Pb plate, the Pb connected to the anode side in an electrolytic cell is oxidized to PbO_2, which acts as the positive active material (PAM). Currently, anodic oxidation of Pb is still employed to prepare PbO_2 electrodes [19]. Because the thicknesses of Pb and PbO_2 on Pb plates are rather limited, a Planté cell has a very low energy density. Due to its simple fabrication method, the LAB was demonstrated to be industrially viable. Therefore, in 1873, the Bréquet Company started to manufacture LAB cells. Then, the electricity generated by mechanical generators could be stored and released by LAB cells. The invention of the incandescent lamp by Thomas Edison marked the advent of the electric era, and electricity entered the everyday life of ordinary people, which increased the demand for LABs. In 1881, Camille Fauré utilized lead oxide paste as the starting material for active materials and invented the paste electrode, a revolutionary technology that increased the energy density of LABs to 8 Wh kg^{-1} [7]. In 1882, Gladstone and Tribe proposed the double sulfate theory of LABs [20]. In the same year, Brush mechanically bonded lead oxide to the plates. Subsequently, in 1886, electrochemically formed Pb and PbO_2 electrodes were designed by Lucas. In 1890, Woodward invented the tubular construction of a PbO_2 electrode, which is a technology we still use today. In 1910, Smith developed slotted rubber tubes to host lead oxides and constructed tubular plates. Expanders (such as lignin, $BaSO_4$, and humic acid) play a fundamental role in present LABs. In 1920, the favorable role of expanders was determined. In 1935, a lead-antimony binary alloy was applied in LAB cells, and Haring and Thomas proved the double sulfate theory, which is the basic principle in the design of LABs. In 1956, Bode and Voss demonstrated the clarification of two forms of PbO_2 (α and β) [21] in the positive electrode. From the 1970s to 1980, sealed valve-regulated lead-acid (VRLA) batteries were developed. By 1990, LABs were widely applied in electric vehicles. In 2004, L. T. Lam invented a supercapacitor-implanted LAB, called ultrabattery. In the 2010s, D. Pavlov and many LAB scientists developed a lead-carbon battery (LCB) for hybrid electric vehicles and renewable energy storage. In summary, although LABs were invented more than 160 years ago, the unique characteristics of LABs make them valuable and allow them to occupy a large market share of rechargeable batteries. LABs are now facing both scientific and technological challenges in emerging applications. Technological

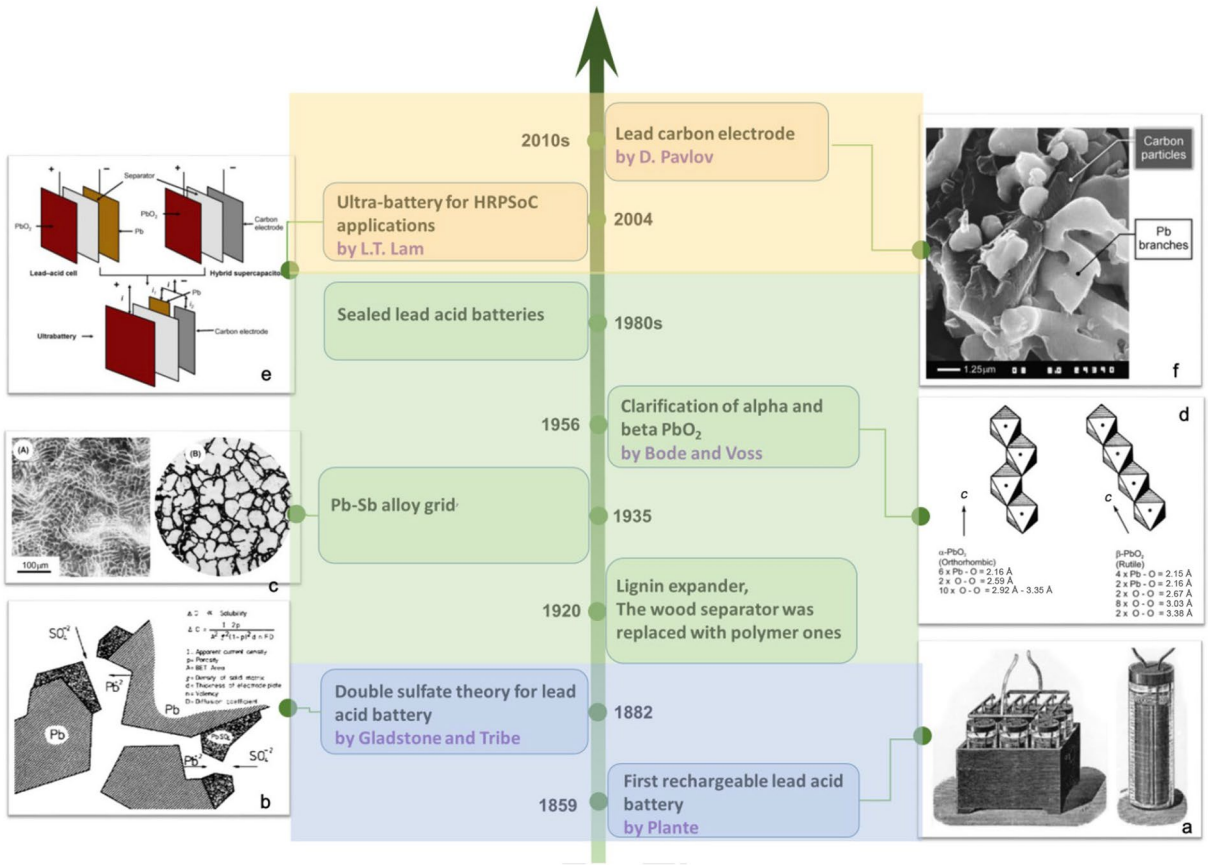

Fig. 1 The development history of LAB technology. **a** A sketch illustrating the architecture of LABs invented by Gaston Planté in 1859. Currently, the spiral design is still used by LAB factories. Reproduced with permission from Ref. [7]. Copyright © 2017, Elsevier. **b** The sulfation process of a Pb negative electrode when Pb is discharged; the PbO_2 electrode also faces sulfation during the discharge process, and the discharge of LABs experiences a double sulfate chemical reaction. Reproduced with permission from Ref. [22]. Copyright © 1977, Elsevier. **c** Grain boundaries and an SEM image of a Pb-Sb alloy grid. Reproduced with permission from Ref. [23]. Copyright © 2017, Elsevier. **d** The structures of α- and β-PbO_2. 1 Å = 1×10^{-10} m. Reproduced with permission from Ref. [24]. Copyright © 2017, Elsevier. **e** A schematic showing the working principle of an ultrabattery. Reproduced with permission from Ref. [25]. Copyright © 2006, Elsevier. **f** An SEM image showing the continuous lead-carbon structure. Reproduced with permission from Ref. [26]. Copyright © 2006, Elsevier

Table 1 Milestones of the LAB development history

Year	Inventor	Historical events and technical advancement
1859	Planté	The Planté cell was invented by transforming Pb into PbO_2 in an electrolytic cell containing H_2SO_4
1880	Gladstone and Tribe	Double sulfate theory was proposed
1882	Brush	Lead oxide was mechanically bonded to plates
1886	Lucas	Lead electrodes were formed in aqueous electrolytes
1890	Woodward	Tubular construction of positive electrodes
1910	Smith	Slotted rubber tube, Exide tubular construction
1920	–	Expander development and machine manufacturing of LABs
1935	Haring and Thomas	Experimental proof of double sulfate theory
1935	–	Lead antimony alloy grid
1956	Bode and Voss	Clarification of two forms of PbO_2 active mass
1970s	McClelland and Devit	Sealed spiral-wound LABs
1980	GNC, USA; YUASA, Japan	VRLA battery technology
1990	–	LABs for electric vehicles and the invention of the bipolar LAB
2004	L. T. Lam	Ultrabattery for hybrid electric vehicles
2010s	D. Pavlov et al.	Lead-carbon electrodes and batteries

advancements will make LABs more attractive for potential applications.

1.2 The Failure Mode of Lead Acid Batteries (LABs) under Partial State of Charge (PSoC)

Generally, the traditional applications of LABs can be classified into four user modes. (1) In UPS applications, in most of its lifetime, an LAB is in the fully charged state, and the LAB faces infrequent discharge. (2) For SLI applications, the LAB is discharged to provide the current for the start and ignition; thus, the LAB faces frequent low-depth discharge. (3) Hours' long charge-discharge cycles with high depth of discharge (DoD) for low-speed electric vehicles. (4) Emerging applications that require the LAB to work under a partial state of charge (PSoC), such as hybrid electric vehicles and the grid-scale energy storage of electricity generated by renewable energy.

In theory, an LAB has limited power performance and short-cycle life due to the intrinsic double sulfate phase-transition mechanism of Pb negative and PbO_2 positive electrodes [Eqs. (1), (2)] [27–29].

$$Pb + H_2SO_4 \leftrightarrow PbSO_4 + 2H^+ + 2e^-, \quad (1)$$

$$PbO_2 + 2H^+ + H_2SO_4 \leftrightarrow PbSO_4 + 2H_2O. \quad (2)$$

Since $PbSO_4$ has a much lower density than Pb and PbO_2, at 6.29, 11.34, and 9.38 g cm^{-3}, respectively, the electrode plates of an LAB inevitably expand during the discharging process. The repeated charge and discharge cycles cause variation in the volume of active material and a decline in the electrode (especially PbO_2) performance. In most of their traditional applications, LABs are operated under full charge-discharge and float charge, which implies that the active materials of both the positive (PbO_2) and negative (Pb) electrodes are constantly charging. In the twenty-first century, the primary challenge for the LAB is its application in HEVs and renewable energy storage, where LABs need to operate under PSoC [7, 30], and other emerging applications, where LABs cannot be fully charged by routine methods [31]. A PSoC duty means that the LAB is not fully charged during its whole operation life. In addition, a PSoC guarantees that an LAB has enough charging and discharging power (Fig. 2a) and can be charged with an unexpected harvest of braking energy in HEV applications (Fig. 2b). Most importantly, the demand for clean and sustainable energy has hindered many countries worldwide from developing renewable energy for future green grids (Fig. 2c). The generation of electricity from renewable energy (such as solar, wind, and tide) is transient and occasional, where batteries play an increasingly important role in transforming transient electricity into highly stable electricity, meaning LABs and LAB modules (Fig. 2d) would operate under

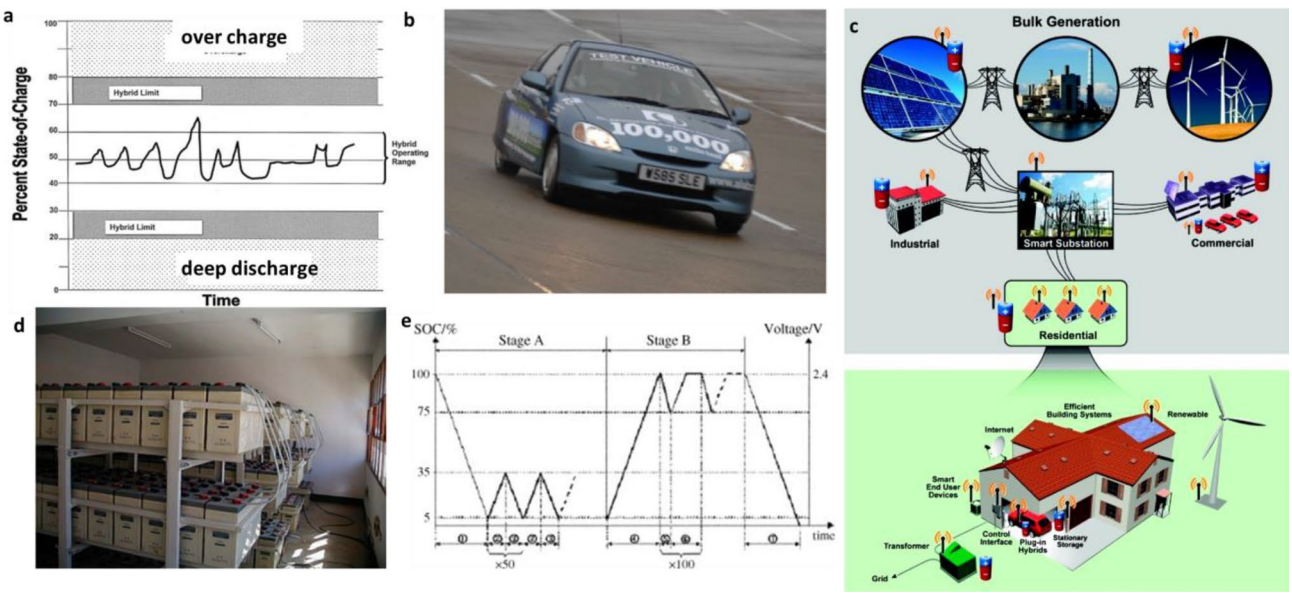

Fig. 2 **a** Dependence of the SoC on time during the operation of batteries in HEVs. Reproduced with permission from Ref. [32]. Copyright © 1999, Elsevier. **b** Honda Insight HEV equipped with advanced LABs. Reproduced with permission from Ref. [33]. Copyright © 2009, Elsevier. **c** Schematic of the application of a green grid that integrates intermittent renewables and hybrid electric vehicles through battery-assisted distribution networks. Reproduced with permission from Ref. [2]. Copyright © 2011, American Chemical Society. **d** 2 V/600 Ah batteries in a battery room for renewable energy storage. **e** IEC 61427 standard cycling test procedure for renewable energy storage. Reproduced with permission from Ref. [34]. Copyright © 2006, Elsevier

PSoC conditions (Fig. 2e) [International Electrotechnical Commission (IEC) 61427: secondary cells and batteries for renewable energy storage—general requirements and methods of test—part 1: photovoltaic off-grid application].

PSoC is an emerging battery operation mode that places higher requirements on LABs than traditional operational applications. Under PSoC conditions, an LAB has a high portion of the discharge product $PbSO_4$ in the negative active material (NAM) [the discharging process is shown in Eq. (3)] [28].

$$Pb + HSO_4^- \leftrightarrow Pb^{2+} + SO_4^{2-} + H^+ + 2e^- \leftrightarrow PbSO_4 + H^+ + 2e^-. \quad (3)$$

The discharge of the Pb negative electrode is performed under a dissolution-precipitation mechanism [28]. Pb is first discharged to soluble Pb^{2+} ions, and subsequently, the Pb^{2+} ions precipitate into $PbSO_4$ crystals. Under PSoC conditions, small $PbSO_4$ particles dissolve and recrystallize into large $PbSO_4$ particles due to the Ostwald ripening process (Fig. 3a) [35, 36]. Operated under PSoC conditions, an LAB either faces numerous high-rate charge and discharge cycles under PSoC in HEVs (i.e., a high rate partial state of charge, HRPSoC) [37] or a long operation time under PSoC in renewable energy storage [38]. Therefore, the accumulation of large $PbSO_4$ particles is exacerbated, and these particles cannot be converted easily due to their low solubility. HRPSoC induces sulfation on the surface of negative plates (Fig. 3b, c). The failure mode related to the formation of large $PbSO_4$ crystals on the surface of the negative electrode is referred to as sulfation.

The low chargeability or charge acceptance of a sulfated Pb negative electrode also induces the parasitic hydrogen evolution reaction (HER) [39] due to the high polarization of the Pb electrode in the charging process. Sulfation does not occur only under PSoC conditions [35]. However, the sulfation of Pb negative electrodes becomes a severe problem when LABs are operated under PSoC for a long time or under high current densities [36]. Sulfation results in the low charge acceptance of the Pb negative electrode, high-voltage polarization during charging, the loss of water from the electrolyte, and a sharp decrease in the reversible capacity. Although the discharge products of both Pb and PbO_2 are $PbSO_4$, compared with the Pb negative electrode [specific surface area (SSA) of 0.5–1.0 $m^2\ g^{-1}$], the PbO_2 positive electrode hardly experiences sulfation (Fig. 3d) due to its large SSA (3.0–8.0 $m^2\ g^{-1}$) [40]. The aggregation of small colloid PbO_2 particles in the PAM could probably enhance the distribution of $PbSO_4$ within the PbO_2 matrix after discharge [3, 41].

The sulfation of Pb negative electrodes has become a prominent obstacle impeding the development of LABs in emerging PSoC applications. Under PSoC, the conventional

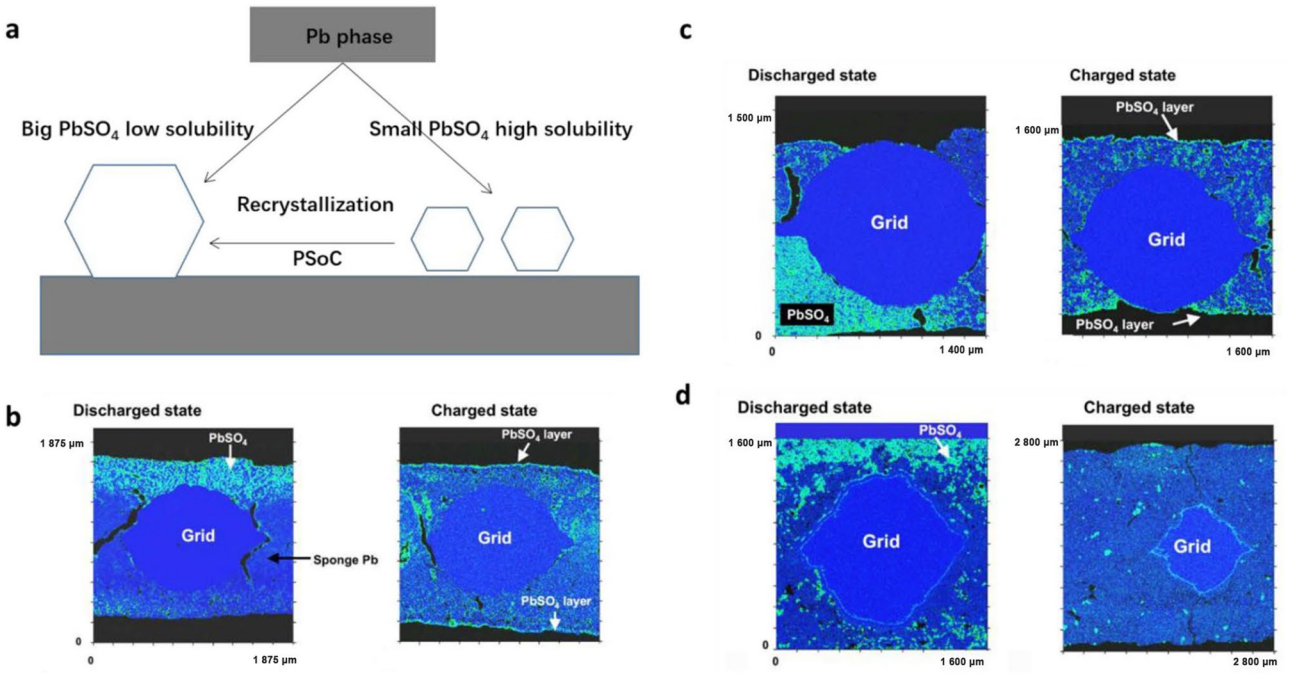

Fig. 3 **a** Schematic illustrating the sulfation process of the Pb negative electrode during HRPSoC operation. Distribution of lead sulfate at the **b** central top and **c** central bottom of a negative plate taken from a failed VRLA battery. **d** Distribution of lead sulfate at the central bottom of a positive plate taken from a failed VRLA battery. Reproduced with permission from Ref. [39]. Copyright © 2004, Elsevier

failure modes of the positive grid corrosion and softening of PbO_2 PAM that occur under the deep charge and discharge of LABs from the full SoC are no longer the major failure modes [39]. Therefore, the charge acceptance and reversible capacity of Pb negative electrodes need to be improved due to the severe sulfation of Pb negative electrodes in LABs operated under PSoC conditions. Since 2005, various methods, such as electrolyte engineering [42], light grid fabrication [43], and architectural design [44], have been employed to enhance the performance of LABs under PSoC. However, these methods can only retard the sulfation of Pb negative electrodes. With the rapid advancement of supercapacitor technology and carbonaceous-based materials for various electrochemical power sources [45, 46], carbon materials have played an increasingly important role in LAB technology [47, 48]. There is an emerging technology called the LCB [49], fabricated by adding functional carbon additives to the NAM of LABs. As a result, the performance of LABs under PSoC conditions has been significantly enhanced. Hence, these carbon-enhanced LABs are now commonly called LCBs. The terminology of LCBs was first proposed by Pavlov [36]. Although the LAB still dominates the medium to large rechargeable battery markets, it is facing significant challenges ranging from traditional applications to PSoC applications. Furthermore, LABs face challenges from low-cost LIBs ($LiFePO_4$/graphite cells). Currently, LCBs are being widely investigated by a large portion of the LAB community, including scientific institutes and companies. Thus, it is necessary to summarize the latest achievements in mechanistic investigation, additive manufacturing, battery manufacturing, full cell evaluation, and practical applications.

In this review, the technological evolution of the LCB is first introduced. Subsequently, the focus is placed on the mechanistic understanding of the lead-carbon binary electrode, the impact of carbon additives on the performance of LCBs, the industrial development of lead-carbon additives for commercial LCBs, and the design of the PbO_2 positive electrode toward long-lived LCBs. In addition, solutions are proposed for the future development of maintenance-free valve-regulated LCBs. Finally, the direction of future research is proposed. As a critical review of LCBs, the technological aspects of the manufacturing of LCBs, such as grid casting [50], pasting [51], acid spraying, curing [51], formation [36, 52], failure modes in different specific applications [53], and operational conditions [54], are not included. This review provides a synopsis and serves as a signpost for the scientific and engineering communities of LABs and LCBs.

2 From Lead Acid Batteries (LABs) to Lead-Carbon Batteries (LCBs)

2.1 PbO_2/Activated Carbon (AC) Asymmetric Electrochemical Capacitors (AECs)

An LAB is composed of a Pb negative electrode and a PbO_2 positive electrode (Fig. 4a). The discharge products of both Pb and PbO_2 are $PbSO_4$. The cycle life and charge acceptance of an LAB under a PSoC is predominantly limited by the sulfation of the Pb negative electrode [55]. Basically, the power capabilities of rechargeable batteries are usually limited by their slow electrode kinetics, while supercapacitors have high charge acceptance due to their nonphase-transition double-layer capacitor charge storage mechanism. Commercial supercapacitors are mainly electric double-layer capacitors (EDLCs) that utilize highly porous activated carbon (AC) (SSA > 1 500 $m^2\ g^{-1}$])as electrode material [56]. Benefitting from their EDLC charge storage mechanism, supercapacitors have higher energy efficiency and charge and discharge rates than rechargeable batteries. The high chargeability of supercapacitors enhances the charge acceptance of Pb negative electrodes. A straightforward solution is to utilize an AC-based paste electrode as the negative electrode and an LAB PbO_2 electrode as the positive electrode (Fig. 4b) [57]. Such a configuration can totally prevent the sulfation of Pb on the negative electrode, which greatly enhances the cycling stability and power performance of energy storage devices based on PbO_2 positive electrodes.

The design principle of a PbO_2/AC asymmetric electrochemical capacitor (AEC). Generally, PbO_2/AC AECs can be fabricated with a thin-film electrode [59, 60] and a thick paste electrode [57]. The design of a thin-film electrode helps to provide high-power capabilities, while that of a thick electrode helps to provide high energy densities. Therefore, with the use of a thick electrode design in an LAB [61], a PbO_2/AC AEC can achieve high energy densities. Additionally, there is motivation to design high-power PbO_2/AC AECs with electrodeposited PbO_2 thin-film electrodes [62, 63]. Regardless of the configuration used, PbO_2/AC AECs can achieve a limited energy density of only 20 Wh kg^{-1} owing to the limited capacities of AC materials and the relatively low specific capacity of PbO_2. PbO_2 restricts the cycle life of a PbO_2/AC AEC due to its phase conversion mechanism. In common cases, PbO_2 is overused (low DoD), and hence, a positive electrode with a long cycle life can be guaranteed. In addition, a hybrid electrolyte composed of 0.1 M (1 M = 1 mol L^{-1}) CH_3SO_3H + 0.1 M $Pb(NO_3)_2$ + 4 M $NaNO_3$ can be employed to enhance the cycling stability [58] because

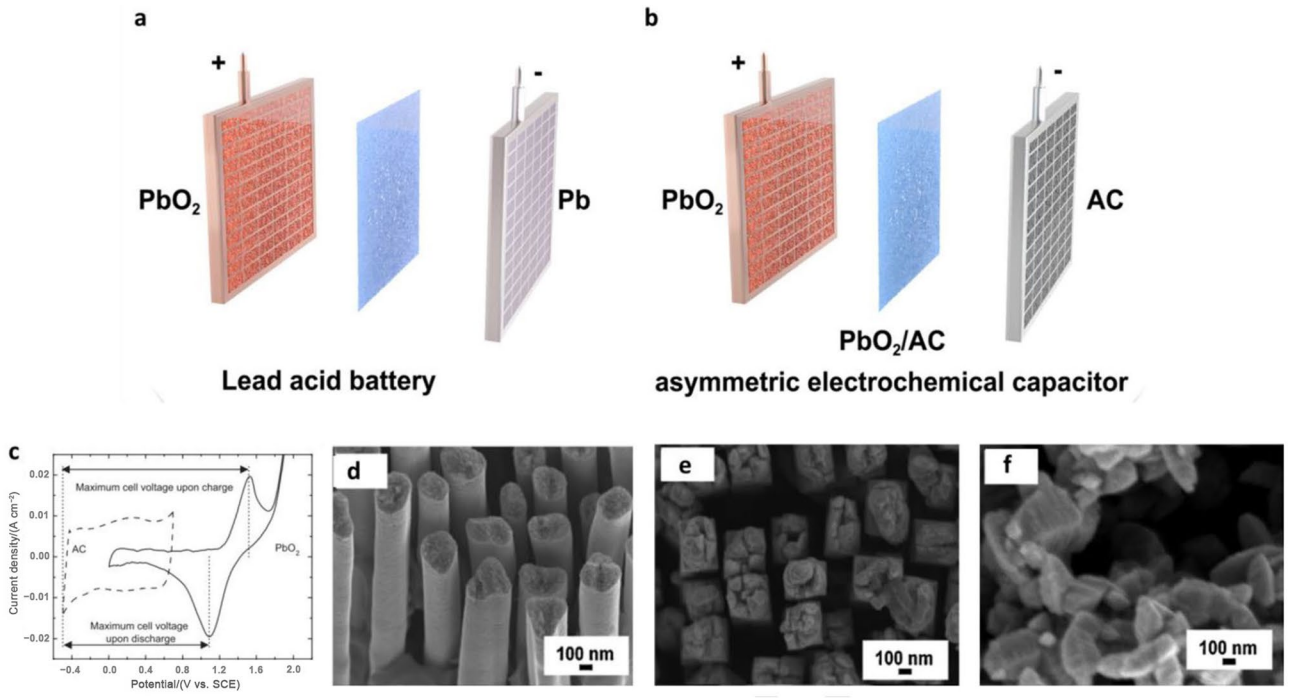

Fig. 4 Configurations of **a** an LAB and **b** PbO_2/AC AEC. **c** Cyclic voltammograms of AC electrodes and PbO_2 nanowire electrodes in a combined 0.1 M CH_3SO_3H + 0.1 M $Pb(NO_3)_2$ + 4 M $NaNO_3$ electrolyte at 10 mV s^{-1}, and SEM images of **d** as-deposited PbO_2 nanowire electrodes and those after **e** 5 and **f** 100 cycles. Reproduced with permission from Ref. [58]. Copyright © 2011, Elsevier

Pb(II) is soluble in this electrolyte combination, which enhances the reversibility of the PbO_2 electrode (Fig. 4c). Nevertheless, the PbO_2 positive electrode faces structural and morphological changes during repeated charge-discharge processes (Fig. 4d–f). PbO_2/AC AECs can be employed as high-power energy storage devices for electrical power management. A superior advantage of PbO_2/AC AECs lies in the low working potential of the AC negative electrode [−0.5 V vs. saturated calomel electrode (SCE)] [58, 60] (Fig. 4c), which enables a high maximum voltage upon charging of 2.4 V. From a technical perspective, the fabrication challenge of PbO_2/AC AECs is the current collector for the AC electrode because a highly corrosive H_2SO_4 solution is utilized as the electrolyte. For thin-film designs, Pb-based alloys may not be suitable as current collectors due to the softness of Pb. Therefore, titanium coated with inert $SnO_2 + Sb_2O_5$ intermediate layers has been used as a current collector for PbO_2 electrodes in many studies [60, 62–65]. The use of PbO_2/AC AECs in high-power applications is promising due to their relatively high power density. However, technical obstacles exist, such as the need for durable PbO_2 positive electrodes and stable negative current collectors.

2.2 Ultrabatteries

Another derivative of LABs is called the ultrabattery, which was designed to replace an energy storage module of externally combined LABs and supercapacitors by an LAB scientist, Dr. L. T. Lam, from the Commonwealth Scientific and Industrial Research Organization (CSIRO) of Australia [25, 66, 67]. Ultrabatteries are fabricated by modifying the traditional components of LABs. The positive electrode is PbO_2, while the negative electrode is Pb replaced by half of an AC paste electrode. Figure 5a presents the current flow when an ultrabattery is charged and discharged. This AC-coated Pb electrode design is expected to reduce the current density of the negative electrode, thus mitigating the sulfation of the Pb electrode. In the detailed architecture of the negative electrode, the traditional Pb electrode is coated with an AC-film electrode. Because AC has a lower hydrogen evolution potential than Pb, in such a design, the AC can operate in a much higher potential range than Pb (Fig. 5b), which implies that AC does not contribute to the current redistribution in the discharging process. Moreover, only a small potential range in the charging process is utilized to alleviate the charge distribution of the Pb negative electrode. At the end of the charging process, the AC electrode faces serious HER,

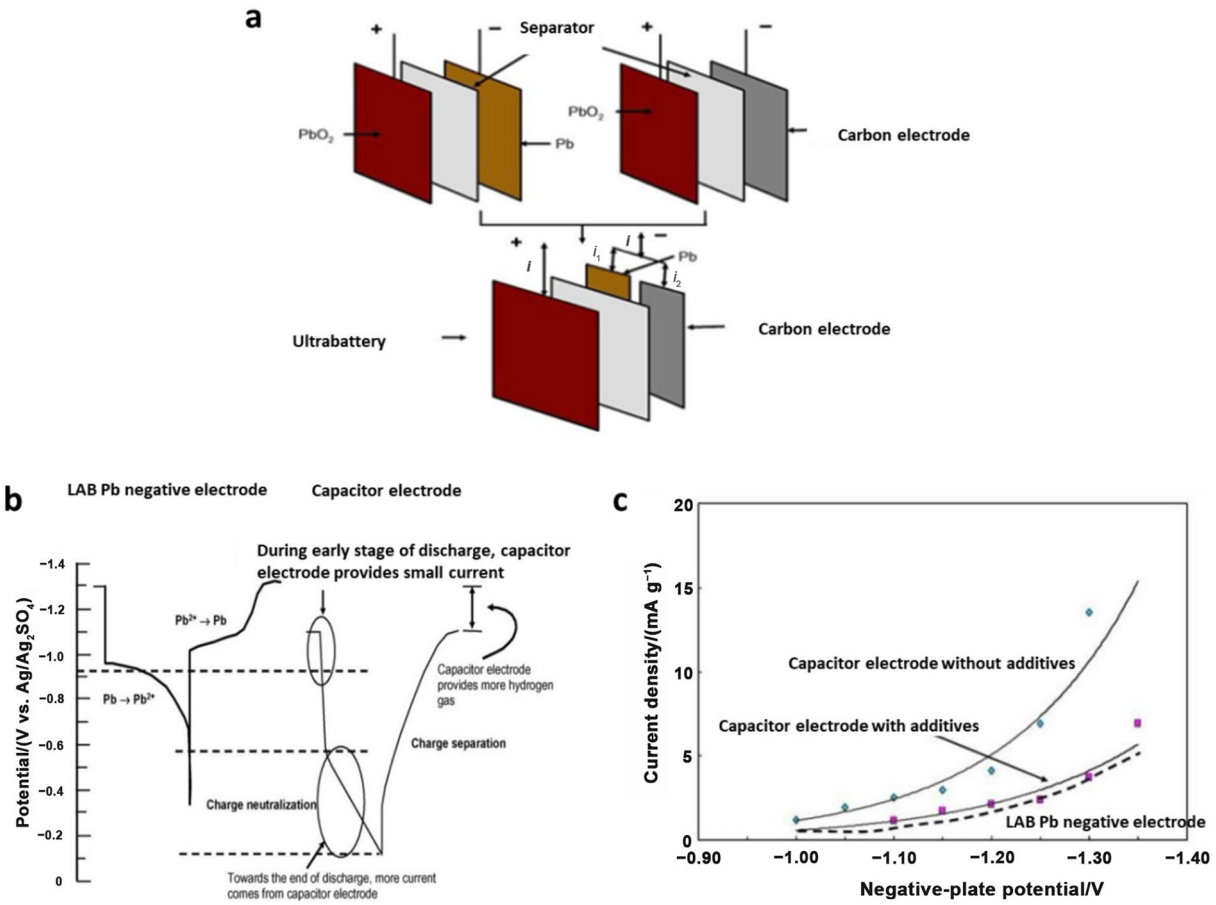

Fig. 5 **a** Configuration of an ultrabattery. **b** The operation potential of Pb negative electrodes and AC electrodes during charging and discharging processes. **c** The steady-state polarization curve of AC electrodes, AC electrodes with additives, and sponge Pb negative electrodes. Reproduced with permission from Ref. [25]. Copyright © 2007, Elsevier

which is avoided in ultrabattery design. As a result, various HER inhibitors, including Pb, PbO, and $PbSO_4$, are added to the AC paste layer. Pb, PbO, and $PbSO_4$ can also contribute to the capacity of the AC electrode. Because Pb has a high HER overpotential, the addition of Pb species can widen the operation potential range of the AC-based composite layer (Fig. 5c). Another category of HER inhibitors includes various metal or metal oxides (Bi, Zn, Ga, In, and their metal oxides) with high HER overpotentials. As a result, the AC layer is not a pure EDLC but a bifunctional EDLC-Faradaic electrode. The detailed design of the ultrabattery can be found in an international patent [67]. In such a design, the composite layer can also alleviate the current distribution in the discharging process, thus providing a more homogeneous distribution of $PbSO_4$.

In Ultrabatteries, a large quantity of AC materials are used in the NAM. In addition, the architecture is so complex that it results in a high manufacturing cost of 500 USD kWh^{-1}, which is higher than the 150 USD kWh^{-1} of flooded LABs and the 200 USD kWh^{-1} of VRLA batteries [2]. The structure of the Ultrabatteries also places high requirements on manufacturing because there is no AC pasting process in a traditional LAB factory. The adhesion force between Pb and AC and inside AC electrodes also needs to be improved for stable negative electrodes.

2.3 Lead-Carbon Battery (LCB)

A more general and simpler method is to modify current LAB technology. AC can effectively enhance the charge power of a Pb negative electrode. If a parallel connection design of Pb with AC is transformed into an inner parallel connection (Fig. 6), namely, the sponge Pb dendrites and AC particles are randomly connected in the NAM, the LAB is transformed into an advanced LAB with a carbon-enhanced bifunctional lead-carbon composite negative electrode [6]. These lead-carbon electrodes have enhanced power and cycle life under PSoC operation, and hence, LAB batteries with lead-carbon electrodes are now commonly called LCBs [26, 49]. The sulfation of LABs can be addressed

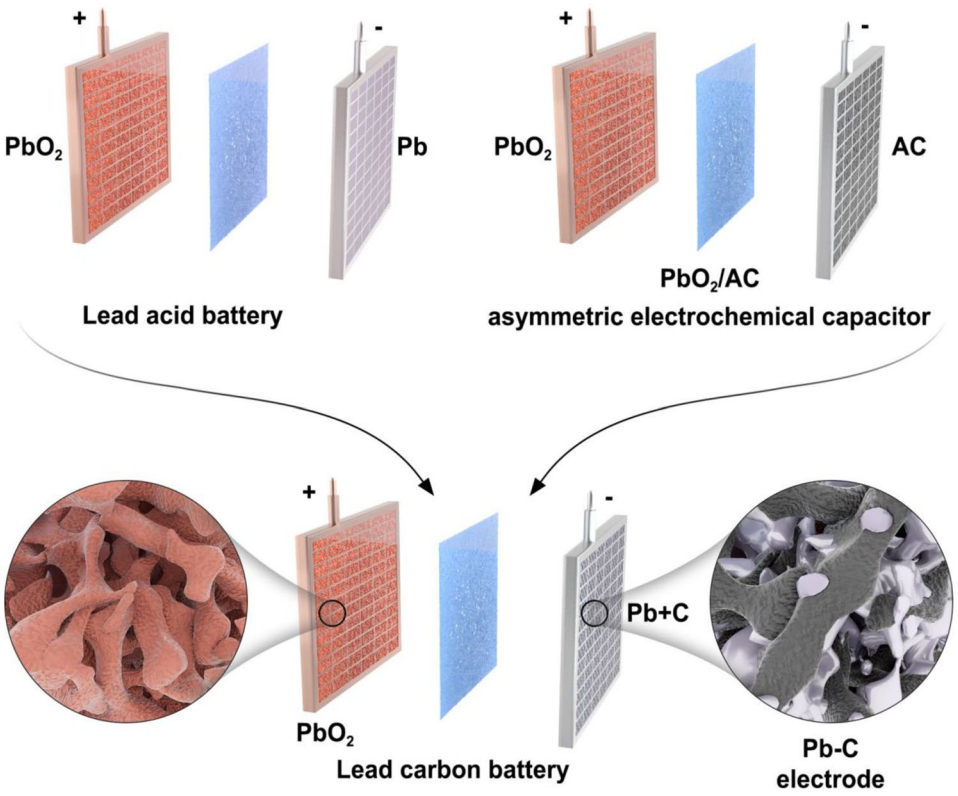

Fig. 6 Configurations of **a** an LAB, **b** a PbO_2/AC AEC, and **c** an LCB. An LAB is composed of a Pb negative electrode, a PbO_2 positive electrode and a separator in the H_2SO_4 electrolyte. A PbO_2/AC AEC is composed of a PbO_2 positive electrode, a Pb negative electrode, and a H_2SO_4 electrolyte. An LCB is composed of a PbO_2 positive electrode, an internally mixed binary Pb-C negative electrode and a separator in the H_2SO_4 electrolyte

with the addition of functional carbon materials, which can increase the conductivity of negative plates and the steric hindrance effect that separates the growth of $PbSO_4$ particles, providing an extra active surface for Pb energetic branch growth [48]. Most importantly, the total capacitance can be enhanced by adding ACs with large SSAs. The inner structure of lead-carbon negative electrodes can be regarded as a parallel connection of Pb with AC at the microscale (the inset in Fig. 6); this is a micro-ultrabattery negative plate. Due to the similarity between lead-carbon composite electrodes and the negative electrodes of ultrabatteries, LCBs face the same issues as ultrabatteries in the charge-discharge process, such as parasitic HER, self-discharge, and electrode expansion.

The utilization of AC is motivated by its high specific capacitance [33, 36, 68, 69], while it has been demonstrated that in the operational potential of a Pb electrode, AC does not contribute to the capacitance of the lead-carbon electrode [6]. The enhanced charge acceptance of a lead-carbon electrode was also achieved by adding other nonporous carbonaceous materials [carbon black (CB), carbon nanotubes (CNTs), graphene, and carbon nanofibers] [70–73] with low SSAs. For this reason, various carbon materials can be used as additives in lead-carbon electrodes. The exposure of the carbon in the microstructure of lead-carbon to the electrolyte can induce parasitic HER such as that in an Ultrabatteries. Therefore, HER inhibitors (such as Zn [74], Ga [75], Bi [76], In [77], and Pb [78]) should be employed to slow the water loss of electrolytes. Of note, a high affinity between lead and carbon components is essential in the establishment of a robust lead-carbon binary composite electrode. Nevertheless, the lead-carbon composite electrode is more complicated than expected, although its components are very simple. In many studies, extensive endeavors have been devoted to the design of a robust lead-carbon electrode for renewable energy storage and HEVs.

In the next section, the mechanistic study and technological advancement of lead-carbon electrodes are thoroughly reviewed. In addition, large-scale synthesis strategies of lead-carbon composite additives that have the potential to be used in the NAM of commercial LCBs are proposed.

3 Roles of Carbon Materials in the Lead-Carbon Negative Electrode

The Pb negative electrode is formed by the electrochemical reduction of basic lead sulfate salts prepared by the mixture of leady oxide and dilute sulfuric acid solution [79] or lead sulfate [80]. After formation, the Pb negative electrode exhibits sponge characteristics with abundant micron-sized lead branches and pores [81, 82]. The smaller and outer layers of Pb branches are more active and energetic, which implies that these Pb branches can be charged

and discharged. The inner Pb branches act as secondary current collectors in addition to Pb-alloy-based grids. Due to the large (microscale) sizes of these Pb branches, sponge NAM has a relatively low SSA ($< 1\ m^2\ g^{-1}$). In addition, after discharge, $PbSO_4$ with a higher volume than Pb grows among Pb branches and recrystallizes into large particles. The discharging process further decreases the SSA of the NAM, which is one reason for the lower utilization of Pb (ca. 50%). Because Pb is a soft metal material, it is difficult to maintain a large SSA and a highly porous structure. Therefore, various NAM additives, or so-called expanders in industry, such as lignosulfonate [83–85], CB, polymer fibers, and humic acid, are employed to sustain its large SSA during repeated charge-discharge cycles [86, 87]. Nanosized $BaSO_4$ particles, as seeds of $PbSO_4$, are employed to distribute $PbSO_4$ and to decrease the size of the $PbSO_4$ [88–90]. In terms of a lead-carbon electrode, the situation becomes more complex; the microstructure and the electrode process have been changed due to the addition of an extra-large amount of carbon material. Various studies have empirically concluded that LCBs show a greatly enhanced cycle life under HRPSoC conditions. Nevertheless, the intrinsic mechanism of carbon materials is still unclear.

In the following section, the functions of carbon materials are classified, and the latest achievements are reviewed. Specifically, the functions of carbon materials are empirically summarized as conductivity improvement, steric hindrance, capacitance contribution, and the electrocatalytic effect [47]. In addition, the synergistic effects of these functions are summarized. Afterward, the main considerations are proposed for the development of high-performance lead-carbon electrodes.

3.1 Conductivity Improvement

The enhanced addition of CB additives (> 0.2% in mass fraction) is actuated from the application of LABs in HEVs that undergo HRPSoC conditions. In 2003, engineers from the Yuasa battery company and Hino motors from Japan found serious sulfation phenomena on the negative plate of LABs in HEV applications [91]. Carbon fibers can enhance the charge acceptance of Pb negative electrodes [73, 95]. Carbon fibers can increase the conductivity of NAM (Fig. 7a) [91], although some researchers believe that carbon nanofibers cannot be evenly distributed in NAM [88]. The addition of CB and graphite may not show the same function of improving conductivity. A small amount of CB can

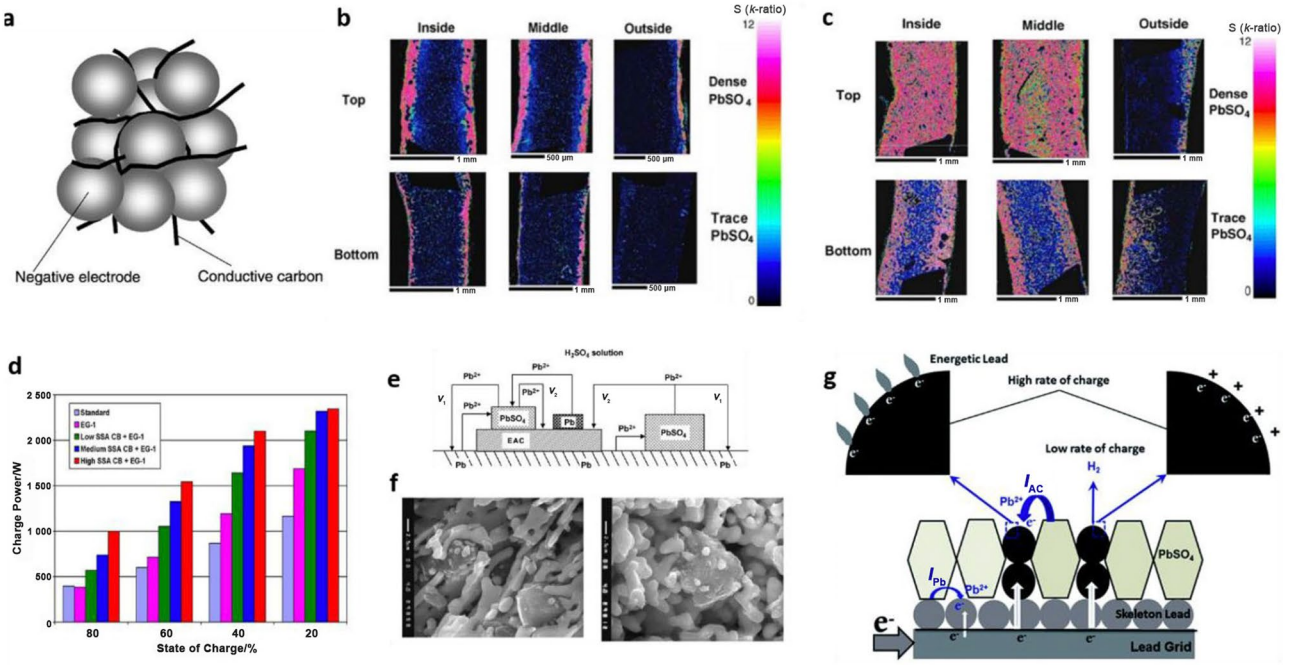

Fig. 7 A summary of the mechanisms of carbon materials in a binary lead-carbon electrode. **a** Conductive pathways built by carbon fibers in the NAM of LABs. Reproduced with permission from Ref. [91]. Copyright © 2003, Elsevier. The $PbSO_4$ distribution (mapped by the sulfur) across negative plates **b** without and **c** with carbon additives after long-term HRPSoC cycling. Reproduced with permission from Ref. [70]. Copyright © 2009, Elsevier. **d** The influence of the charge power with different carbon additives in the NAM. Reproduced with permission from Ref. [92]. Copyright © 2010, Elsevier. **e** The parallel reaction mechanism of lead deposited on carbon and Pb surfaces. Reproduced with permission from Ref. [93]. Copyright © 2009, Elsevier. **f** Morphology of Pb dendrite growth on the surface of AC. Reproduced with permission from Ref. [94]. Copyright © 2011, Elsevier. **g** Electrochemical processes in the charge process of a lead-carbon composite electrode. Reproduced with permission from Ref. [6]. Copyright © 2015, Royal Society of Chemistry

effectively enhance the conductivity, while a large amount of graphite can prominently enhance the conductivity [96]. The different behaviors of different carbon additives may be caused by the different densities, particle sizes, and microstructures of CB and graphite [97]. CB contains nanosized particles that can form continuous conductive pathways on the surface of Pb, which can enhance the conductivity. High-density graphite can be separated in NAM, which results in a noncontinuous distribution. CB [97–99], graphite [70, 92], CNTs [72, 100–103], vapor-grown carbon fibers [95], AC [36, 75, 93, 94], and graphene [104–107] can provide conductive pathways based on the specific amounts added. Although Pb has a high conductivity of 4.85×10^4 S cm^{-1}, which is much higher than that of most carbonaceous materials, carbon materials can enhance the overall conductivity of NAM composed of a certain portion of $PbSO_4$. Note that in a conventional LAB, CB is employed as a conductive agent, with a common addition ratio of CB of 0.2 wt% (weight percentage ratio). In LCBs, the optimized addition amount of CB and other carbon materials can be increased to 2.0 wt% or above [108–110]. Due to the diversity of carbon allotropes and the chemical structures of carbon materials, there are also variations in the optimal amount of added carbon materials. Therefore, it is necessary to conduct optimization experiments to determine the optimal amount of one certain carbon material [94].

3.2 Steric Hindrance

Moseley proposed that a higher SSA increases the cycling stability of lead-carbon electrodes that operate under HRPSoC conditions [33]. Because a higher SSA is beneficial to the distribution of $PbSO_4$ particles, it can alleviate sulfation. Graphite, TiO_2 particles, glass fibers, AC, and Al_2O_3 can effectively enhance the porosity and SSA of NAM [111, 112]. In addition, these additives can separate the growth of $PbSO_4$ particles. However, from a historical perspective, SSA and porosity have not been regarded as important parameters in research on LABs. Micka found that graphite and TiO_2 can play the same role of prolonging the HRPSoC cycling life of LABs [111]. Because TiO_2 serves as an insulator, graphite can function in the same role as TiO_2 through a steric hindrance effect. Flaky graphite, expanded graphite (EG), and glass fibers have been explored as additives in NAM. Compared with flaky graphite, EG and glass fibers can enhance the specific surface of NAM, which contributes to higher HRPSoC cycling stability [70]. These additives can enhance the $PbSO_4$ distribution across the negative plate. In HRPSoC operation, a high current density induces the growth of compact $PbSO_4$ on the surface of negative plates of LABs (Fig. 7b, c). Compact $PbSO_4$ can hinder the diffusion of HSO_4^- anions into the NAM, which induces high polarization and low charge acceptance during charging. Křivík proposed that graphite impedes the growth of $PbSO_4$ [112], but it cannot be excluded that graphite contributes to the active sites for the deposition of Pb. A large SSA is important because it can provide abundant active sites for the growth of Pb and the separation of $PbSO_4$, which is beneficial to the charging process. Nevertheless, the positive roles of TiO_2 verify the steric hindrance effects of particulate additives in NAM.

3.3 Capacitance Contribution

ACs with large SSAs can provide high double-layer capacitance, which contributes to the charge accumulation and distribution of the Pb electrode. In a binary lead-carbon composite electrode structure, AC is embedded in the Pb architecture, and thus, on the microscale, an AC particle can be regarded as a micro-ultrabattery electrode. Moseley calculated the contribution of AC in a lead-carbon electrode to HEV application. AC (25 wt%) is required to provide capacitance [33]. However, on the one hand, it is difficult to incorporate a large amount of AC into NAM due to the density difference between carbon and leady oxide [48]; on the other hand, in most reports, the mass loading of carbon additives in NAM is limited to only 1–3 wt% but has a significant enhancement effect on the charge power of lead-carbon electrodes. For instance, Fernández investigated the dependence of the charge power on the SoC [92]. He found that in a wide range of charging states, an optimized lead-carbon electrode based on an AC additive has a higher charge power than a Pb negative electrode (Fig. 7d). Based on the significant effects of carbon materials, Pavlov proposed a new terminology, i.e., the LCB [36]. In a binary lead-carbon system, the particle size of the carbon materials and the affinity of AC to lead architecture (lead affinity) are significant parameters. The particle size of the carbon has an impact on the distribution of carbon materials in NAM, while a high affinity can determine the formation of continuous lead-carbon interfaces [48]. However, the electrical connection of Pb and carbon inside the NAM of LCBs results in irreversible HER, which not only causes water loss from the electrolyte but also destroys the continuous Pb architecture in NAM.

3.4 Electrocatalytic Effect

Since the capacitive contribution should not contribute to the capacity in the charging process, enhanced charge acceptance should be induced by the reduction of $PbSO_4$ on carbon materials. In the late 1990s, Kozawa proposed the electrocatalytic effect of carbon materials in NAM [99]. However, Kozawa did not propose any evidence that Pb was electrodeposited on carbon. Pavlov found the formation of Pb on the carbon surface and proposed the electrochemical reduction of $PbSO_4$ on the carbon surface. As a result,

a parallel electrolysis reaction mechanism was proposed (Fig. 7e, f) [93, 94]. In this parallel reaction mechanism, the reduced current on carbon is much higher than that on the Pb surface, which results in a significant enhancement of the charge power with a limited carbon addition (~2 wt%). Our group have started research on LCBs since the work of electrodeposited PbO_2 electrodes for electrochemical energy storage [62] and PbO_2/AC AECs [60]. Subsequently, a study was performed on LCBs in practice in an attempt to explore the electrochemical deposition behaviors of Pb on the AC surface with various electrochemical and physicochemical methods [6]. AC was selected on the grounds that AC has both a large SSA and an electronically conductive crystalline structure. It was found that the capacitance of AC can be negligible in the charging process. In contrast, the deposited Pb on AC has a low polarization compared with that on Pb and provides a very high capacity. The deposited Pb on AC surfaces is determined by the surface area and geometry of the AC. Therefore, it can be proposed that AC functions as an electron distributor that is conducive to the growth of three-dimensional (3D) energetic Pb branches (Fig. 7g), which is the major electrochemical origin for the enhanced charge acceptance of lead-carbon electrodes [6]. Due to the catalytic role of carbon and the 3D growth of Pb branches, this role is defined as "electrocatalytic deposition and 3D growth". Small micropores do not allow Pb to be deposited inside, while mesopores and macropores can enable the deposition of Pb [113]; hence, the pore size of carbon materials plays an important role. Note that the depolarization effect of carbon materials may result from irreversible HER and electrocatalytic Pb deposition on carbon. Therefore, the depolarization of lead-carbon electrodes compared with a Pb electrode cannot be employed to quantify the effects of carbon addition.

3.5 Comprehensive Mechanistic Understanding of Carbon Additives

There has been continuous work on lead-carbon binary electrode systems and persistent mechanistic studies. It is necessary to present a clearer picture of the lead-carbon composite electrode (Fig. 8a). In this review, a comprehensive explanation of the carbon components in lead-carbon electrodes is presented. Various carbon materials can contribute to the establishment of the architecture of NAM, in which micron-sized large carbon particles, such as graphite and AC, are incorporated into the architecture of Pb NAM, thus achieving no contribution to the conductivity. Carbon materials with small particle sizes and high aspect ratios contribute to conductive pathways by forming a continuous electron pathway from the inner to the outer surfaces of the NAM. Various carbon materials can enhance the SSA of NAM, which alleviates sulfation through the formation of small $PbSO_4$ particles due to steric hindrance. If carbon materials are exposed to the H_2SO_4 electrolyte, Pb grows on the surface, which also contributes to the electrochemically active surface area for reversible Pb deposition. These Pb particles grow on the carbon surface and act as secondary energetic Pb branches, which enhances the utilization of NAM [110]. Therefore, carbon with a high affinity to Pb deposition is significant in the establishment of a binary lead-carbon microstructure [114, 115]. In this way, carbon can enlarge the SSA of NAM, which can achieve a result similar to that of traditional expander additives, such as lignosulfonate, $BaSO_4$, and polymer fibers. Distinct from traditional expanders, carbon materials act as electrochemically active surfaces for Pb deposition. Hence, the improvement in the SSA of the Pb negative electrode is so significant that it needs to be further explored with respect to LCBs [116].

Due to the distinct role of carbon materials, the affinity of carbon materials to Pb deposition is so significant that it needs precise investigation. It is easy to find that different types of carbon possess different affinities for Pb deposition through simple SEM investigation [115]. Quantifying the influence of the microstructure of carbon materials on the deposition process of Pb is difficult but of significance. There remain many scientific issues regarding the mechanism of Pb deposition on carbon. First, how can the affinity of different carbon materials to Pb deposition be quantitatively measured [114]? Second, can a carbon powder electrode or a carbon powder emulsion electrode exhibit behavior representative of a lead-carbon binary electrode system or not [117]? Third, do defect sites enhance the deposition of Pb on the carbon surface, and what are the roles of oxygen functional groups and heteroatoms [114]? Settelein et al. investigated the nucleation dynamics of Pb on two different graphite materials [EG and synthetic graphite (SG)] from a Pb^{2+}-containing electrolyte [114] (Fig. 8b–h). They directly incorporated EG and SG in a real-world Pb negative electrode and found that EG provided a much better connection to the surrounding Pb matrix than SG (Fig. 8b, c). The ultimate goal of this research is to determine whether Pb plays an important role in incorporating carbon materials into NAMs. They investigated the nucleation role of EG and SG with overpotentials of 100 and 200 mV with a deposition charge of 100 mAs cm^{-2} (Fig. 8d, e). It is clear that EG provides many more nucleation sites than SG per unit area (Fig. 8d, e). Figure 8f presents the dependence of the nucleation sites on the overpotential based on the chronoamperometric model. To determine the structure-performance relationship of the deposition of Pb and the properties of carbon materials, they investigated many physicochemical properties of EG and SG materials, including impurities, SSAs, crystalline sizes, particle sizes, pH values, and contact angles. They concluded that the only reasonable way that lead can bond to the carbon surface is via active

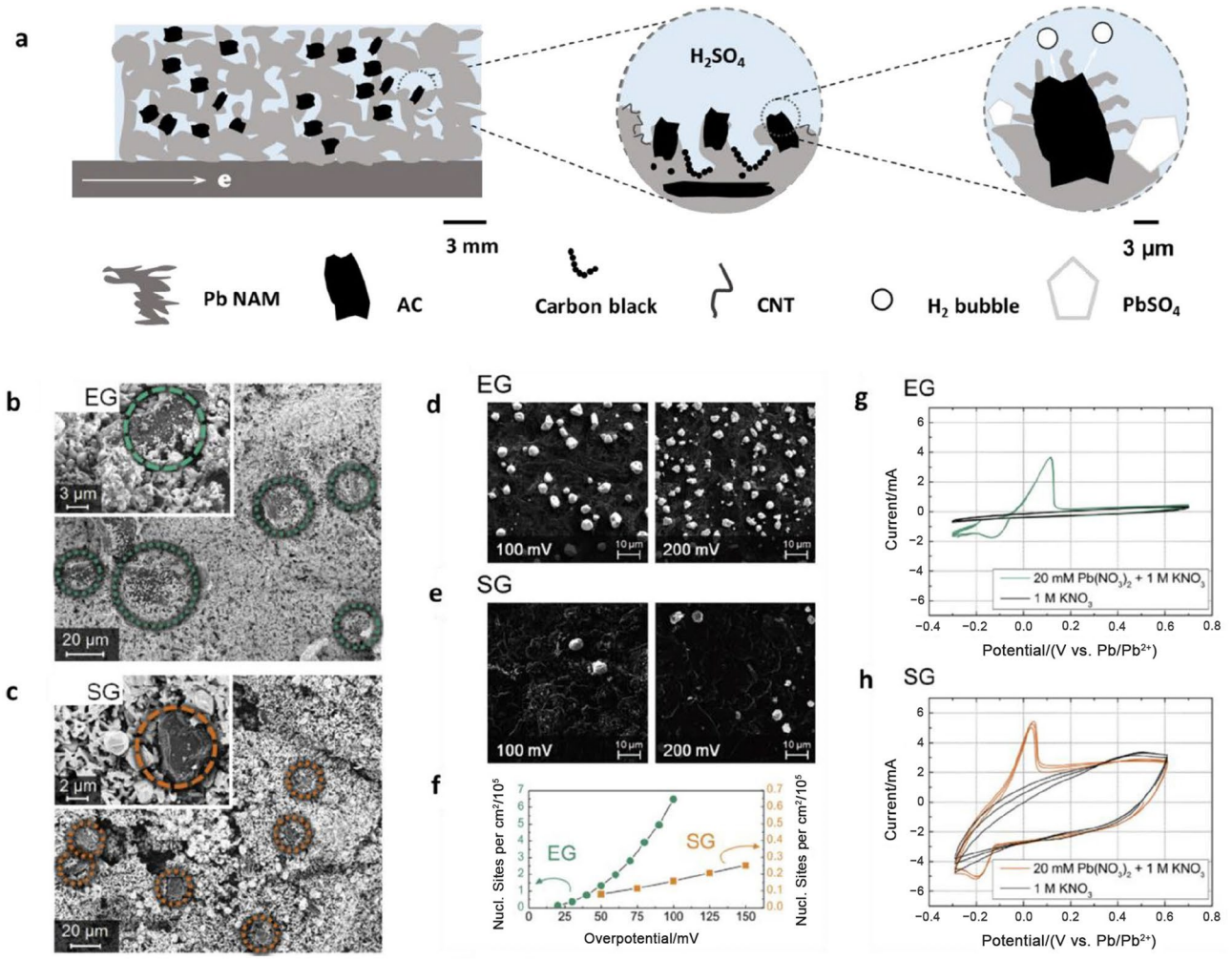

Fig. 8 **a** Schematic illustrating the structure of a binary lead-carbon electrode from the millimeter scale to the microscale. SEM images of the NAMs with **b** EG and **c** SG as carbon additives. SEM images of lead electrodeposited on **d** EG and **e** SG at a total transferred charge of 100 mAs cm^{-2}, **f** the relation between the number density of nucleation sites and the overpotential of both EG and SG materials, cyclic voltammograms of **g** EG and **h** SG in 1.0 mol L^{-1} KNO_3 aqueous solution with and without 0.02 mol L^{-1} lead nitrate. Reproduced with permission from Ref. [114]. Copyright © 2017, Elsevier

sites at step edges and kinks. The above theory is consistent with the simulated deposition of Pb in a Pb^{2+}-containing electrolyte (Fig. 8g, h), in which the EG electrode exhibits a much higher Pb plating/stripping current than the SG. The edge site and surface functional groups likely play an important role. More work should be performed with the aim of understanding the precise role of defects in catalytic deposition. Of note, the 3D architecture of a lead-carbon electrode with carbon additives with strong catalytic effects should be investigated.

The incorporation of carbon in the Pb architecture can induce adverse effects such as the HER [118], electrode expansion [113], and self-discharge. These three side effects are detrimental to the operation of a full battery. Carbon has a much lower overpotential for the HER than Pb [118]. Therefore, in LCBs, inhibiting the HER and building continuous, robust lead-carbon electrodes are of equal significance. Several practical methods for producing carbon-based additives that have the potential to be employed in LCBs are proposed.

3.6 Effects of Carbon Additives on the Electrochemical Performance of Lead-Carbon Batteries (LCBs)

It has been demonstrated that AC additives are efficient in the sulfation inhibition of Pb negative electrodes [119]. Normally, in a traditional LAB, the addition of CB in the NAM of LABs is controlled to 0.2 wt% with respect to the mass of leady oxide. NAM with a small amount (normally < 2 wt%) of functional carbon additives is defined as a lead-carbon electrode. LABs assembled with lead-carbon

negative electrodes are defined as LCBs. When nanosized CB is employed as an additive, the electrochemical behaviors of lead-carbon electrodes are determined by the quantity of CB [120]. A traditionally small amount of CB, ca. 0.2 wt%, is located on the surface of the NAM, which provides an extra electrochemical active area for Pb deposition. A large amount of CB, ca. 2 wt%, can easily aggregate, which deteriorates the cycling stability of lead-carbon electrodes. Special techniques, such as spray drying, can be employed to homogeneously mix CB and leady oxides [121]. Different from CB with nanosized particles, microsized carbon materials such as AC and graphite can act as conductive architectures inside NAM [94, 96, 122]. Carbon additives with large SSAs play important roles in promoting the kinetics of lead-carbon electrodes. During formation, Pb^{2+} ions can deposit on the large electrochemically active surface area that is provided by carbon additives and generate Pb nuclei [89, 115]. Carbon additives with mesopores and hierarchical pores are more conducive to Pb deposition than microporous carbon. Mesopores and macropores can provide sufficient space for Pb^{2+} ion transportation and the growth of lead branches [123]. Because the Pb growth on the carbon surface plays a significant role, the affinity between carbon additives and Pb is another important factor of carbon additives [94, 115, 124]. However, it is difficult to detect and evaluate the physical affinity between Pb and carbon. Various electrochemical methods can be utilized to characterize the affinity of some carbon materials to Pb deposition. Settelein et al. reported that EG with more defects shows a higher affinity for lead than graphite [114]. Carbon materials with abundant defects, such as EG, reduced oxide graphene, amorphous CB and AC, show a favorable affinity for Pb deposition [123]. Because the majority of these carbon materials have a particulate morphology, approaches that expose the active defect sites should be explored in research on LCBs.

AC has been widely investigated because it strongly enhances the power of Pb negative electrodes in HRPSoC applications. In addition, the preparation of AC in industry is rather mature, and the physicochemical characteristics can be tracked. In later research, it can be demonstrated that the high porosity of AC is highly effective for the performance enhancement of lead-carbon electrodes. Xiang et al. reported that AC in a Pb negative electrode can increase the HRPSoC cycle life of LCBs (Fig. 9a) [68]. Various studies have reported varying numbers for HRPSoC cycle lives due to the different manufacturing processes, cell configurations, and carbon additives used in different laboratories around the world. To demonstrate the feasibility of LCBs for HRPSoC operations, it is necessary to follow factory manufacturing procedures for the production of LCB cells designed for

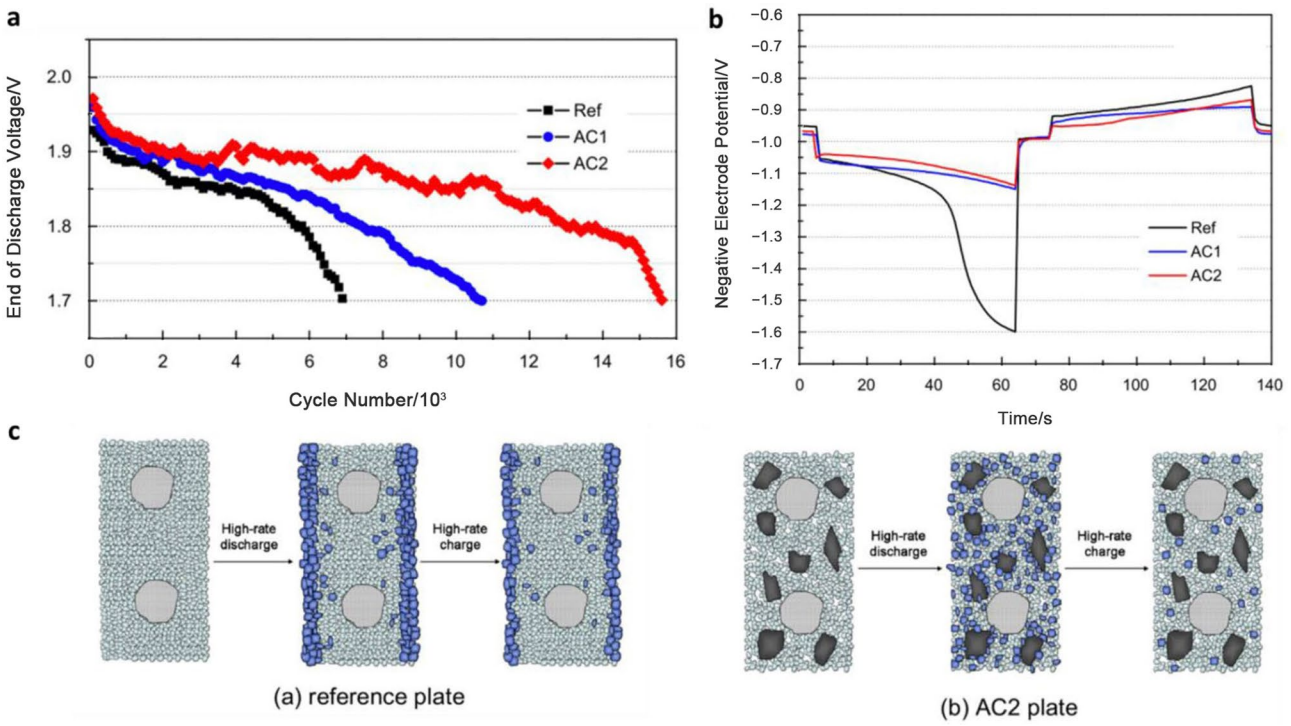

Fig. 9 **a** HRPSoC cycling performance of LABs and LCBs with different AC carbon additives: the dependence of the cell voltage on the cycle number. **b** Potential-time curve of the negative electrode during one HRPSoC charge-discharge cycle. **c** Schematic illustrating the Pb negative plate with and without AC additives after long-term HRPSoC cycling. Reproduced with permission from Ref. [68]. Copyright © 2013, Elsevier

real-world applications. Compared with the control battery, the LCBs with AC in the negative electrode show much lower polarization due to the capacitive buffering effect of AC (Fig. 9b). AC particles with a size of tens of microns can act as a conductive architecture and catalyze the lead deposition and dissolution reactions in the inner part of the lead-carbon electrode, which alleviates the sulfation of NAM (Fig. 9c). The depolarization effects of AC can also originate from the HER. Therefore, the rate of H_2 evolution should be evaluated with quantitative collection methods.

The HER is a parasitic reaction of the negative electrode in the lead-carbon electrode of LCBs [36]. Because carbon materials usually exhibit low HER overpotentials, the addition of carbon materials can accelerate the HER rate of a lead-carbon negative electrode [47]. Therefore, a lead-carbon electrode shows a higher HER rate than a Pb negative electrode [125]. A high HER rate cannot be tolerated in a VRLA design in that H_2 gas cannot be consumed inside the battery tank like oxygen. Normally, carbon additives with higher SSAs can provide more reaction active sites for the HER [116]. Undesirable HER reduces the energy efficiency, decorates the structure of the NAM, and consumes the water in the electrolyte. Inhibiting the HER is required to achieve high-performance LCBs with a long cycle life.

The addition of soluble HER inhibitors to electrolytes can decrease the HER rate of lead-carbon electrodes. Benzaldehyde derivatives [126], polyaspartic acid [36][36], 1-ethyl 3-methylimidazole diethyl phosphate (EMDP) [127], L-serine [128], and boric acid [129] have presented satisfactory effects for HER inhibition in the negative electrode of LABs. However, these additives apparently cannot decelerate the HER rate of the lead-carbon electrode. In addition, these electrolyte additives may change the properties of the interphase between the electrode and the electrolyte. Of note, PbO_2 can also oxidize these organic additives in electrolytes in long-term cycles [63]. Deyab et al. investigated the effect of 1-ethyl-3-methylimidazolium diethyl phosphate (EMIDP) on suppressing the HER [127]. Although the HER rate is decreased, the EMIDP adsorbed on the surface of the Pb negative electrode can cause an increase in the charge transfer resistance and a decrease in the double-layer capacitance. Additionally, surface chemistry modification of the carbon additive is regarded as an efficient method for HER inhibition. Wang et al. confirmed that the species of surface functional groups are related to the HER rate [130]. If carbon additives are modified with acidic surface functional groups, lead-carbon electrodes present a low rate of HER. In contrast, if carbon additives are modified with alkaline surface functional groups, lead-carbon electrodes present a high rate of HER. In addition, doping nitrogen [131] and phosphorus [132] on carbon additives presents HER inhibition effects. Wang et al. investigated the effect of nitrogen doping in carbon additives and demonstrated that nitrogen doping can effectively decrease the HER rate, where the underlying mechanism is that the electronegativity of nitrogen can effectively induce electron deficiency in the carbon architecture [131]. Another method to decelerate the HER rate is to apply metal or metal species with a high overpotential for the HER. In this strategy, zinc [74], indium oxides [77], bismuth oxide [75, 76], and gallium oxide [75] have been shown to increase the overpotential for the HER. Nevertheless, these additives may cause difficulties in the recycling of the lead. In the majority of these studies, researchers use linear scan voltammetry (LSV) to investigate the HER rate; however, the HER is highly dependent on the SoC and the active state of the Pb NAM. The real-time HER rate in constant voltage charging and cycling should be evaluated with quantitative methods.

3.7 Toward Large-Scale Application of Pb-C Based Additives

Lead is a metal with a high HER overpotential. A lead-carbon composite integrated with lead and carbon additives can increase the HER overpotential. The preparation of lead-carbon composites can also increase the densities of carbon additives, which makes paste technology more feasible for LCBs. Due to the high density of leady oxide, lead-carbon additives with high densities can be distributed more homogeneously in lead paste than pure carbon additives with low densities. Moreover, lead is the prominent active component of the lead-carbon electrode. Lead-carbon composite fabrication is conducive to forming a strongly connected lead-carbon interphase, which is beneficial to inhibiting the HER and to constructing conductive networks in lead-carbon electrodes. Therefore, lead-carbon composites instead of carbon additives are more practical in LCBs.

The fabrication methods of lead-carbon composites are crucial for achieving lead-carbon electrodes with low HER rates, high energy efficiency, and high cycling stability. Notably, lead-carbon composites should have particle sizes comparable to or larger than those of lead powder to serve as the architecture of the electrode. The relatively high surface area of lead-carbon composites can provide extra electrochemical surface area for lead deposition and dissolution. The content of lead species should be controllable, with the aim of optimizing the density and the surface area of lead-carbon composites [134]. Additionally, a strongly connected lead-carbon interphase is essential for HER inhibition and a favorable network for the whole electrode [108]. The preparation method should also be simple and easy for large-scale manufacturing. Tong et al. prepared a Pb^{2+} ion-containing AC composite (Pb@C) by combining AC and $Pb(NO_3)_2$ in an incubator shaker [133]. The Pb@C composite shows small Pb particles on the surface of AC (Fig. 10a). Energy-dispersive spectroscopy (EDS) demonstrates that the

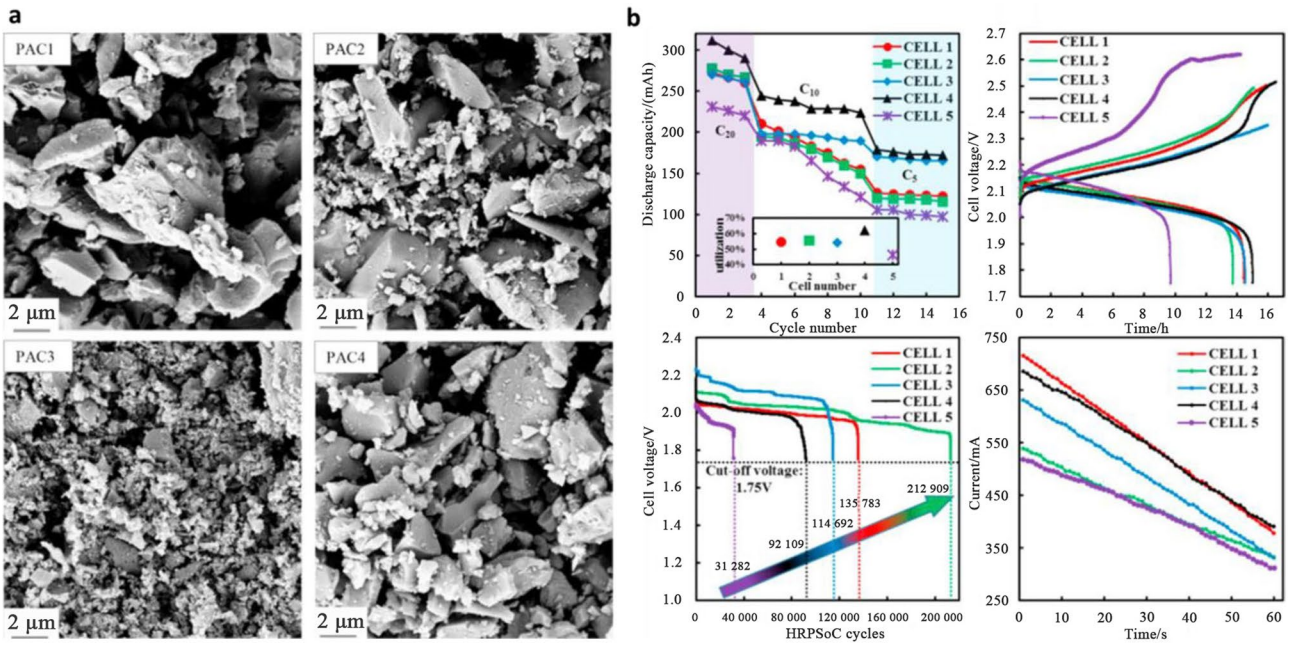

Fig. 10 **a** SEM images of Pb@C additives. **b** Electrochemical performances of lead-carbon electrodes with different additives. Discharge capacities at different rates; charge-discharge curves at a 10 h rate; end-of-discharge voltage during the HRPSoC test; charge acceptance curves tested at 2.55 V. Reproduced with permission from Ref. [133]. Copyright © 2015, Elsevier

Pb species are not evenly distributed. In the LSV test, the Pb@C electrodes present a lower HER current than the AC electrode in the potential range from − 0.6 to − 1.75 V (vs. mercury/mercurous sulfate (Hg/Hg_2SO_4) reference electrode (MSE)). The LCB with the Pb@C additive presents a long cycle life (212 909 cycles) (Fig. 10b), seven times that of the control cell in the HRPSoC test. LCBs with Pb@AC also present higher capacity and charge acceptance than the control cells (Fig. 10b). Hong et al. prepared a nano-lead-doped AC composite (nano-Pb/AC) by ultrasonic adsorption and precipitation [69]. AC and $Pb(NO_3)_2$ were mixed in a solution with the ultrasonic method. Subsequently, $PbSO_4$ was precipitated on the surface of AC by dipping in a dilute H_2SO_4 solution. The lead loading mass ratio of nano-Pb/AC is ca. 3.32 wt%. After ultrasonic adsorption and precipitation, the nano-Pb/AC presents a surface area of 1 192 $m^2\ g^{-1}$, which is lower than that of AC (1 528 $m^2\ g^{-1}$). The nano-Pb/AC electrode presents a lower onset potential of the HER (−1.14 V) than the AC electrode (− 1.02 V). The nano-Pb/AC composite also enhances the charge acceptance and NAM utilization of the lead-carbon electrode. Similarly, Zhang et al. prepared a layered carbon/$PbSO_4$ composite by soaking layered carbon in a $Pb(NO_3)_2$ solution with the addition of H_2SO_4 [135]. The layered carbon was prepared with a chemical vapor deposition method. The layered morphology of the carbon can effectively distribute the $PbSO_4$ species and form a layered structure [135]. In the discharging process, $PbSO_4$ can be reduced to Pb located between carbon layers. This layered design is conducive to distributing carbon in the NAM of LCBs and to reducing the HER rate. The above preparation methods have the merits of achieving high surface areas and homogeneous lead distribution on the surface of lead-carbon composites. However, lead-carbon composites fabricated by Pb^{2+} ion adsorption can obtain only a limited amount of lead. In addition, the above methods cannot guarantee a strongly connected lead-carbon interphase between lead species and carbon. A strongly connected lead-carbon interphase is necessary for inhibiting the HER and for constructing favorable networks of lead-carbon electrodes.

Pyrolysis can induce the carbon reduction reaction of PbO, which can generate a stable Pb-C interface. Yang et al. prepared a PbO@C composite by pyrolyzing lead citric acid [49]. The as-prepared PbO@C composite presents a moderate surface area of 264.0 $m^2\ g^{-1}$ and an in situ formed lead-carbon interphase. When used as the additive of the NAM, the PbO@C composite improves the utilization of NAM from 56.9% to 72.5%. The lead-carbon cell with the PbO@C composite presents a long HRPSoC cycle life, four times that of the control cell. Wang et al. prepared a lead-doped mesopore-dominated carbon (Pb@MC) composite by electrodepositing lead on the surface of mesoporous carbon [136]. The lead particles achieve a favorable connection with the mesoporous carbon through the electrodeposition method. Transmission electron microscopy (TEM) images indicate that the amount of deposited lead does not increase

due to the nanoconfinement effect of the mesopores. Thus, when used as an additive in the lead-carbon electrode, the Pb@MC composite not only presents a favorable effect on HER inhibition but also provides extra capacity through the nanolead. Although the Pb@MC composite is a favorable additive for lead-carbon electrodes, the electrodeposition method is time-consuming and complex for large-scale manufacturing.

Our group prepared an oxygen-deficient lead-carbon (rice-husk-based hierarchical porous carbon (RHHPC)@PbO_{1-x}) composite with a sol-gel method in combination with pyrolysis treatment (Fig. 11a) [108]. The sol-gel method with pyrolysis treatment is simple and suitable for large-scale manufacturing. The as-prepared RHHPC@PbO_{1-x} composite is homogeneously coated with nano-PbO_{1-x} seeds through scanning electron microscopy (SEM) and TEM (Fig. 11a). These nano-PbO_{1-x} seeds serve as active sites for the 3D growth of Pb branches (SEM images in Ref [108].) and sustain the large SSA of the NAM. The RHHPC@PbO_{1-x} composite possesses a strongly connected lead-carbon interphase, high surface area (1 111.3 $m^2\ g^{-1}$), and large pore volume (0.66 $cm^3\ g^{-1}$). The cell with the RHHPC@PbO_{1-x} composite presents better rate performance than the control cells (Fig. 11b). A 100% DoD test was employed to simulate the severe protocols of renewable energy storage with a low-state charge of 60% and a long-term rest under the discharged state (100% DoD for 5 h) for each cycle.

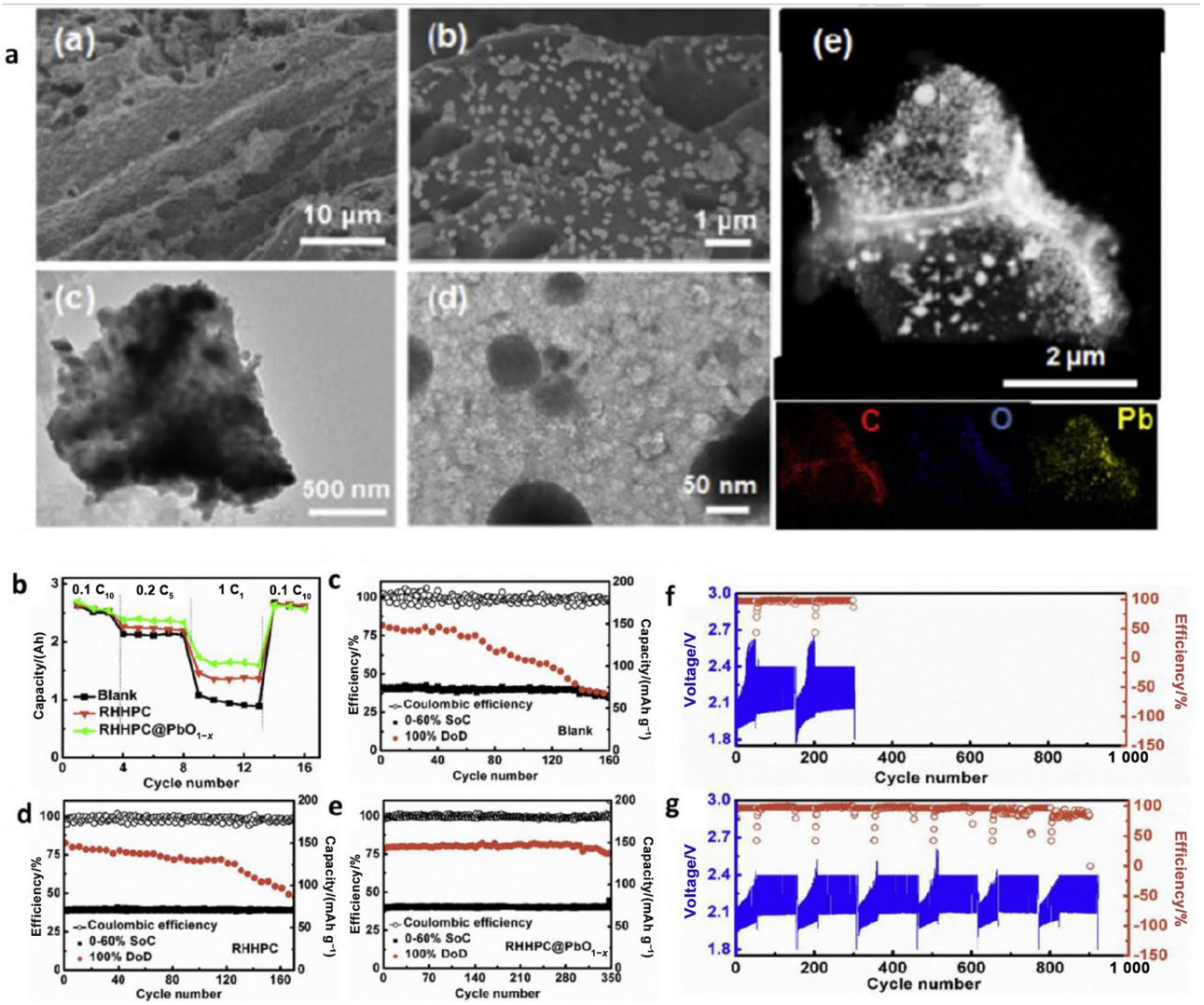

Fig. 11 **a** SEM and TEM characterizations of RHHPC@PbO_{1-x} additives. **b** Rate capabilities of LCBs based on RHHPC and RHHPC@PbO_{1-x} additives. PSoC cycling stabilities for **c** a blank control battery, **d** LCBs with RHHPC, and **e** RHHPC@PbO_{1-x} additives. Cycling stability of **f** the control and **g** RHHPC@PbO_{1-x} LCBs tested by IEC standards. Reproduced with permission from Ref. [108]. Copyright © 2020, Elsevier

Through this cycling test, lead-carbon electrodes with abilities to inhibit sulfation can be quantified. The control cells without carbon additives and with RHHPC additives present capacity retention of 80% after 81 and 136 cycles, respectively (Fig. 11c, d). In comparison, the RHHPC@PbO_{1-x} cell exhibits a high capacity retention of 96.5% after 350 cycles (Fig. 11e). Furthermore, the viability of LCBs with the RHHPC@PbO_{1-x} composite is demonstrated by full cells (4.0 Ah of 10-h-capacity). When the test is conducted according to the IEC standard (IEC 61427:2005) for renewable energy storage, the RHHPC@PbO_{1-x} LCB completes six cycle sets (900 cycles), which is triple that of the lead acid control battery (Fig. 11f, g). This high performance may be caused by the homogeneous distribution of the PbO and robust Pb-C interface. The intrinsic mechanism of this RHHPC@PbO_{1-x} can sustain a large SSA of 6.5 $m^2\ g^{-1}$ of the NAM, while Pb NAM and RHHPCNAM present small SSAs of only 4.07 and 0.5 $m^2\ g^{-1}$ after PSoC cycling. This method is also promising for large-scale manufacturing with the scale-up of the fabrication process of RHHPC@PbO_{1-x}.

4 Toward Long-Life PbO_2 Positive Electrodes in Practical Lead-Carbon Batteries (LCBs)

4.1 Fundamentals of PbO_2 Positive Electrodes

The discharge of a PbO_2 positive electrode is expressed in Eq. (3). The typical discharge mechanism of the PbO_2 electrode involves a proton participation process, which requires the application of proton-containing sulfuric acid as the electrolyte.

$$PbO_2 + HSO_4^- + 3H^+ + 2e^- \leftrightarrow PbSO_4 + 2H_2O. \quad (4)$$

The discharge product of the positive electrode is $PbSO_4$ [Eq. (4)]. Considering the large SSA of PbO_2 (3–8 $m^2\ g^{-1}$) and its colloid-crystal structure (Fig. 12a), PbO_2 can hardly cope with sulfation. PbO_2 contains two kinds of crystalline structures, i.e., α-PbO_2 (orthorhombic) and β-PbO_2 (rutile), both of which exist in the PAM of the positive electrode [41]. The PAM of the PbO_2 positive electrode is a complex mixture of amorphous hydrated zones and crystal zones

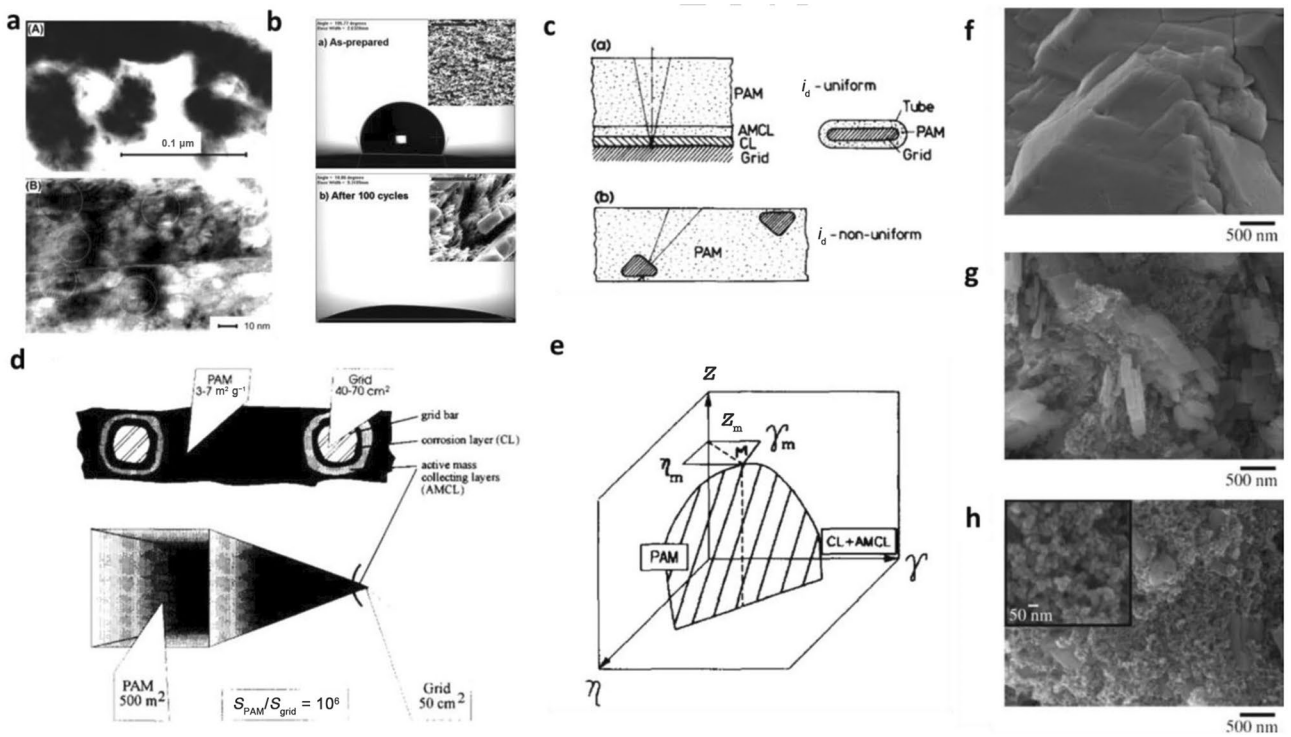

Fig. 12 **a** Crystal-gel microstructure of PbO_2 active materials, with fingerprints indicating the crystal zones. Reproduced with permission from Ref. [24]. Copyright © 2017, Elsevier. **b** Contact angle test of the PbO_2 nanowire electrode before and after cycling. Reproduced with permission from Ref. [137]. Copyright © 2014, Elsevier. **c** The cross-section of the PbO_2 positive electrode illustrates the layered structure composed of PAM, the active mass collecting layer, the AMCL, the corrosion layer, the CL, and the grid. Panel **c** also shows the different cross-sections of tubular, grid, and planar positive plates. **d** The specific surface parameters of the positive plates. **e** The relationship of Z, η, and γ. Reproduced with permission from Ref. [40]. Copyright © 1995, Elsevier. Morphologies of electrodeposited PbO_2 electrodes, **f** as electrodeposited, **g** after 10 cycles, and **h** after 200 cycles in 4.7 mol L^{-1} H_2SO_4 aqueous electrolyte. Reproduced with permission from Ref. [138]. Copyright © 2011, Elsevier

(Fig. 12a), which facilitates the proton and electron conductivity of PbO_2 [139, 140]. Therefore, a thermal dehydration process may degrade the capacities of PbO_2 electrodes [141, 142]. In terms of both crystalline structures of PbO_2, β-PbO_2 can provide high capacity, while α-PbO_2 can serve as the architecture of the PAM. Both α-PbO_2 and β-PbO_2 can exist in chemically or electrochemically formed PbO_2 [60, 62, 137, 143], while the connection between PbO_2 particles plays an important role in exhibiting their electrochemical capabilities [19, 144, 145]. A highly crystalline PbO_2 electrode can present a low initial capacity due to the hydrophobic nature of the surface [138]. Activation cycling can transform a hydrophobic surface into a hydrophilic surface (Fig. 12b) [137].

Commercial PbO_2 PAM generated by the formation of leady oxide paste [tribasic sulfate (3BS) or tetrabasic sulfate (4BS)] is naturally amorphous, which is essential to fully utilizing its capacity [146]. On the one hand, the accumulation structure of PbO_2 particles with hydrate zones can cause long-term softening of the PAM, which hampers the cycling stability of PbO_2 electrodes; on the other hand, additive engineering of PbO_2 can minimally improve the performance of PbO_2 electrodes [147–151] due to the high oxidation characteristics of PbO_2. Therefore, the design of the architecture of the PbO_2 electrode (planar, tubular, and grid) and microstructure (generated from 3BS or 4BS) is of significance (Fig. 12c). A critical parameter of the PbO_2 electrode is the current distribution, through which planar and tubular electrodes can effectively decrease the local current density and the Pb grid can induce a high local current density. Pavlov proposed several parameters to describe the influence of design parameters on the performance of PbO_2 positive electrodes [40]. Parameter γ is employed to describe the importance of the weight of PAM loaded on the grid and the surface area of the grid (Fig. 12d). Thus, $\gamma = W_{PAM}/S_{grid}$, where W_{PAM} represents the weight of the PAM, and S_{grid} represents the surface area of the grid. The other two parameters represent the utilization of the PAM (η) and the cycle life (Z). A three-coordinate system can be established to describe the relationship between the design parameters γ, η, and Z (Fig. 12e). The function passes a peak value at which the cycling stability is controlled by either the PAM or the corrosion layer. Note that the grid alloy composition plays an important role in the corrosion layer. High-resistance alloys are essential for the development of maintenance-free lead-based batteries [43, 152–154]. The PbO_2 positive electrode is a complex system from active materials to interfacial design and requires the optimization of the above parameters and the compatibility of the battery configuration (Fig. 12f). Note that an electrodeposited PbO_2 coating electrode [21, 155] is more compact than chemically formed PbO_2 [143] and an anodically oxidized PbO_2 film [145] due to its continuous and compact structure. Nevertheless, an electrodeposited PbO_2 positive electrode faces a morphological evolution from a compact stone-like structure to a sand-like structure (Fig. 12f–h).

4.2 Recent Progress on PbO_2 Positive Electrodes

Commercial PbO_2 plates are chemically prepared (cured) plates [51] and electrochemically formed in H_2SO_4 electrolytes [52]. PbO_2 exhibits a highly porous structure but inferior cycling stability. To enhance the cycling stability of positive electrodes, most work has been performed on the preparation of 4BS-based pastes [156] or nano-4BS [157] as seeds for the growth of large 4BS crystals in positive pastes. Lei et al. made contributions with $PbSO_4$ as the precursor of the PAM [158], achieving high cycling stability. Because $PbSO_4$ can be employed as the precursor of NAM [80], LABs can be established with an acid-free electrode-making process, which is promising for use as a novel manufacturing technology in the LAB industry. A second popular approach is to enhance PAM integration by adding functional additives [159]. However, carbon additives undergo complete decomposition during cycling, such as CB and biomass-derived carbon [147, 160]. Other mineral additives may degrade the performance of PbO_2 electrodes [161]. Most positive additives introduce or retain more water inside the paste and enhance the utilization of PbO_2 positive electrodes. Therefore, favorable cycling stability can be achieved by architecture design. Electrochemically deposited PbO_2 films can exhibit a long cycling life but possess a low specific capacity due to their compact structure [138]. Therefore, a more open porous nanowire PbO_2 electrode is efficient for both enhancing the utilization of PbO_2 and expanding the cycling stability [162], although the fabrication of PbO_2 nanowires is a complicated template-based method. A PbO_2 nanowire electrode exhibits a compact but open structure after hundreds of cycles [137], while most inorganic additives may exert little impact on the performance of the PbO_2 electrode, especially the cycling stability. CNTs added to the positive paste enhance the cycling stability and PbO_2 electrode capacity [163]. The fabrication of PbO_2 with an electrodeposition method may not be simple in industry; however, the superior cycling stability of these PbO_2 nanowire electrodes may provide a foundation for favorable manufacture of the PbO_2 plate.

5 Toward Advanced Maintenance-Free Valve-Regulated Lead-Carbon Batteries (LCBs)

The VRLA battery is an advanced LAB design. The wide application of LABs is ascribed to the high overpotentials of the HER and oxygen evolution reaction (OER) of the Pb

and PbO_2 electrodes, respectively. Nevertheless, an LAB is a battery system based on an aqueous H_2SO_4 electrolyte and cannot avoid the adverse impacts of the HER and OER on the Pb and PbO_2 electrodes. Although the H_2SO_4 electrolyte is nonflammable, the evolved H_2 and O_2 may pose an explosion hazard. LAB scientists have tried to design a sealed LAB free from the generation of gases. After the failure of the internal catalytic recombination of H_2 and O_2, LAB scientists finally invented VRLA batteries with "gel" electrolytes [169] and electrolytes in the absorbent glass mat (AGM) [164, 170]. The design of VRLA batteries aims to achieve "zero" gas emissions via an "internal oxygen recombination cycle" (Fig. 13a) in these electrolytes. The internal oxygen recombination cycle implies that the O_2 gas evolved from the PbO_2 electrode is consumed on the Pb negative electrode [Eq. (5)].

$$Pb + 1/2O_2 + H_2SO_4 \rightarrow PbSO_4 + H_2O + \text{Heat}. \quad (5)$$

Gas diffusion channels are designed in H_2SO_4 electrolytes for the diffusion of O_2 from the PbO_2 positive electrode to the Pb negative electrode because the diffusion of O_2 through the gas space (diffusion coefficient, 0.18 $cm^2\ s^{-1}$) is much faster than that through the aqueous electrolyte (diffusion coefficient, $9 \times 10^{-6}\ cm^2\ s^{-1}$) (Fig. 13a). Generally, gel electrolytes are formed by the gelling of the H_2SO_4 electrolyte with fumed silica nanoparticles, leaving cracks inside that act as O_2 diffusion channels [171–175]. The AGM technique employs the O_2 generated at the end of the formation to fill in the H_2SO_4-filled AGM, which generates O_2 diffusion channels [176]. Gel and AGM techniques can also be combined to make a composite electrolyte [175]. Gel and AGM VRLA technologies are designed to realize the internal recombination of O_2 [166]. Various cell configurations, such as a planar cell (Fig. 13b), a spiral LAB cell (Fig. 13c), and positive tubular plates (Fig. 13d), can be employed to achieve various performances. Antimony, which has been applied in negative grid alloys, is not applied in VRLA batteries due to its high HER reactivity [54]. In the high-state charge of a VRLA battery, oxygen is consumed at the Pb negative electrode (Fig. 13e), in which the HER is suppressed. Extra oxygen and hydrogen gas is released from a valve into the air. If oxygen recombination is conducted unsteadily, the charging of the Pb negative electrode becomes blocked, and hence, sulfation becomes severe.

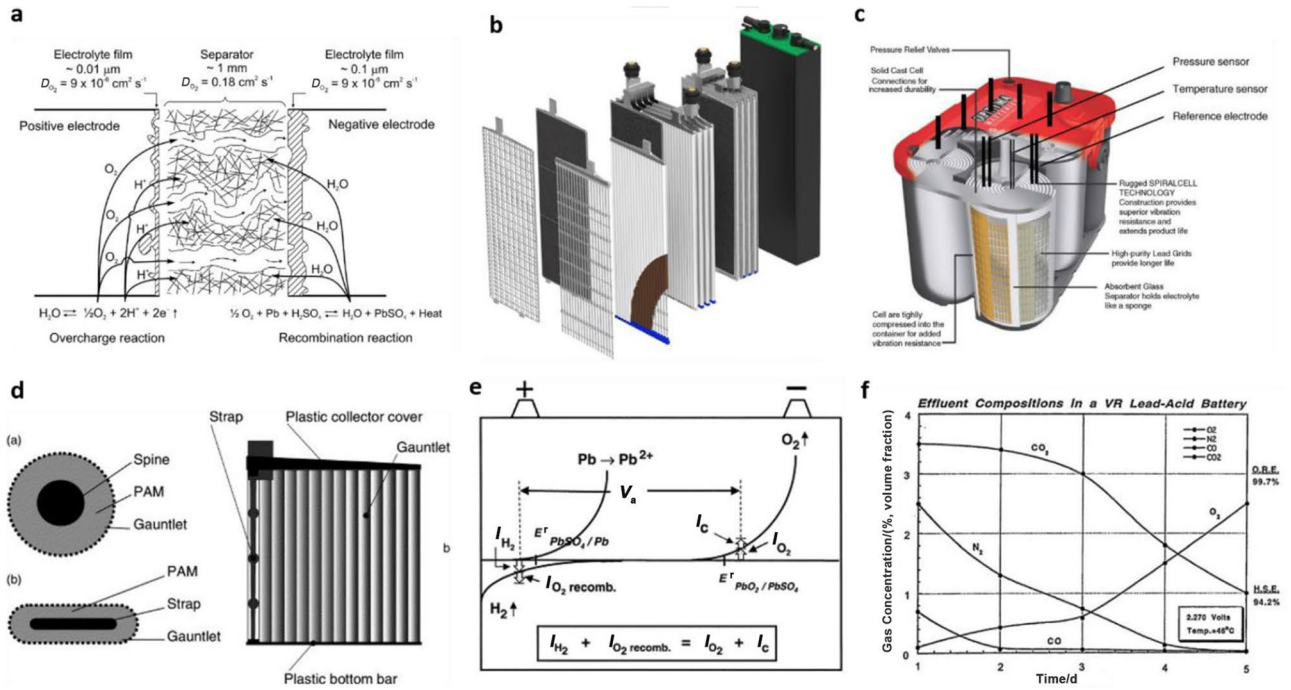

Fig. 13 **a** The architecture and schematic of reactions occurring in the "gel" and AGM electrolytes in VRLA batteries. Reproduced with permission from Ref. [164]. Copyright © 2017, Elsevier. **b** A schematic diagram illustrating the structure of flooded LABs. Reproduced with permission from Ref. [165]. Copyright © 2018, Elsevier. **c** An architecture of spiral LAB cells based on coiling electrode plates. Reproduced with permission from Ref. [166]. Copyright © 2006, Elsevier. **d** Structure of tubular PbO_2 positive plates. Reproduced with permission from Ref. [167]. Copyright © 2003, Elsevier. **e** The potential characteristics of positive and negative electrodes in a VRLA battery under float charging. Reproduced with permission from Ref. [54]. Copyright © 2000, Elsevier. **f** The dependence of the effluent composition (N_2, CO_2, CO and O_2) evolved from a VRLA battery at 46 °C. Reproduced with permission from Ref. [168]. Copyright © 2010, Elsevier

VRLA batteries have been a significant and innovative success for LABs. For LCBs, one consideration is the high HER rate on the lead-carbon negative electrode, and hence, a high HER should be suppressed by HER inhibitors. The other consideration is the oxygen recombination cycle inside a battery tank. The O_2 gas diffusing to the Pb negative electrode not only consumes Pb but also induces the consumption of carbon additives inside the NAM. Due to the introduction of carbon additives in the NAM, the parasitic reactions become rather complicated [168]. Carbon dioxide and monoxide may be formed due to the oxidation of carbon. Competition of carbon with lead for oxygen from the formation of formic acid (HCOOH) reduces the formation of lead sulfate formed by an incomplete oxygen cycle. Figure 13f presents the apparent competition of oxygen and carbon dioxide formation [168]. The significant influence of carbon additives on the recombination of oxygen should be investigated in detail.

6 Application of Lead-Carbon Batteries (LCBs) in Grid-Scale Energy Storage

The traditional applications of LABs can be divided into four categories: (1) infrequent discharge conditions in UPSs. In these applications, LABs are forced to be float-charged most of their service life and can be forced to discharge to support energy consumption only in emergency conditions; (2) frequent, shallow DoD for SLI applications in automobiles. The discharge rates for SLI can reach 20–30 C [177]; (3) deep charge-discharge conditions in low-speed electric vehicles, with discharge rates ranging from 1/3 to 2 C [178]; and (4) the application of LABs working under PSoC conditions. PSoC conditions are present in hybrid electric vehicles [179] and grid-scale energy storage of electricity generated by renewable energy [14, 38]. PSoC is probably the application area of LABs with the most significant advancement in the twenty-first century. For HEVs, due to the limitation of low specific energy density, LABs can be applied only in micro-HEVs. For start-stop HEVs, practical demonstrations of LCBs in real circumstances are important. Practical performances can also provide researchers with guidance for the design of durable LCB full cells for HEVs. In the next decade, there are great opportunities for the design of LCBs for renewable energy storage in harsher environments.

Renewable energy storage resembles RAPS applications. However, the capacity for renewable energy storage is much larger than that of a RAPS. The power capability of these energy storage systems ranges from 100 kW to several megawatts (MW), and the energy storage capabilities range from hundreds of kilowatt-hours to tens of megawatt-hours [170]. LABs have undergone long-term technological evolution in large-scale energy storage applications. In 1986, Southern California Edison constructed the largest LAB energy storage system at that time, which consisted of 8 256 Exide gel batteries in eight parallel strings with each of 1 032 cells (voltage 2 000 V) reaching a 4-h-rate capacity of 40 MWh given an 80% DoD. The warranted cycle life is 2 000 cycles (8 years). This facility was decommissioned in 1997, and the LABs were subsequently recycled.

Advanced LCBs are used in novel renewable energy storage systems; in the Notrees project, wind farm systems were implemented (Fig. 14a) that can achieve the acquired capacity by combining several 1 MW battery units. Its design objective is to resolve the wind power system intermittency with a 36 MW/24 MWh Xtreme Power Inc. battery energy storage system (Fig. 14b). The scope of this energy storage system is the integration of the electricity generated by renewable energy into the local grid system and the enhancement of energy storage during nonpeak generation periods to support grid management. The Kahuku energy storage system is located in Kahuku, Hawaii, USA. The output power of the Kahuku wind farm is 30 MW, with a total annual generation output of 68 000 MWh. This project is coupled with an energy storage system of 15 MWh (Fig. 14c). A lead battery energy storage system was developed by Xtreme Power Inc. An energy storage system of ultrabatteries is installed at Lyon Station Pennsylvania for frequency-regulation applications (Fig. 14d). This system has a total power capability of 36 MW with a 3 MW power that can be exchanged during input or output. It has been demonstrated that this system can achieve 92%–95% DC/DC efficiency in regulation services, with an average AC to AC efficiency of 80%. Because of the high reliability of LCBs, they are receiving increasing attention for large-scale energy storage.

Benefitting from the high reliability and high safety of lead-based rechargeable batteries (Table 2), LABs have been applied to many mature medium- to large-scale energy storage systems for multiple purposes [170]. LABs are specifically characterized by their safety and low cost compared with other battery chemistries. Fortunately, LCBs are not more expensive than LABs due to the limited utilization of carbon additives in the NAM. Because the cost of LCBs is much lower than that of LIBs (Table 2), the energy storage cost of LCBs can be significantly lower than that of LIBs [5, 45].

The energy storage cost of LCBs per cycle based on the capital cost is 0.1 USD kWh^{-1}; however, it would be 0.6 USD kWh^{-1} per cycle for LIBs, which is much more expensive than that of LCBs. In view of the high safety of LCBs, it is recommended that LCBs have priority for large-scale renewable energy storage. However, an energy storage cost of 0.1 USD kWh^{-1} is still high compared to the low cost of coal-generated electricity. Therefore, further engineering methods are required to enhance the cycle life of LCBs and to decrease the energy storage cost per unit of energy [5].

Fig. 14 Energy storage systems based on LAB and LCB systems. **a** Digital picture of the Notrees project wind farm site and **b** 36 MW/24 MWh Xtreme Power Inc. battery energy storage system. **c** 15 MWh Xtreme Power Inc. battery energy storage system at the Kahuku wind farm. Reproduced with permission from Ref. [180]. Copyright © 2017, Elsevier. **d** Ultrabattery energy storage systems for frequency regulation at Lyon Station, Pennsylvania. Reproduced with permission from Ref. [10]. Copyright © 2018, Elsevier

Table 2 Comparison between the technical parameters of LIBs and LCBs

Parameter	LCB	LIB
Energy density	35–40 Wh kg^{-1}	200–300 Wh kg^{-1}
Power density	100–500 W kg^{-1}	800 W kg^{-1}
High operation temperature	40 °C	50 °C
Low operation temperature	−30 °C	−20 °C
Charge acceptance	Good	Better
Cycle life[a]	1 500–2 000	1 000–5 000
Reliability	Proven	Need to be approved
Recyclability	Excellent	Uneconomic
Safety	Excellent	Issues to be solved
Cost per unit energy	150 USD kWh^{-1}	600 USD kWh^{-1}

[a]Cycle life tested at a DoD of 80%. The cycle life of batteries may vary with different DoDs, architectures, and manufacturing technologies

7 Summary, Outlook, and Future Research Directions

7.1 Summary of Lead-Carbon Battery (LCB) Technologies

Currently, LCBs are an increasingly important rechargeable battery system in emerging applications that are operated in the PSoC mode. There is no doubt that LCBs are more complex than LABs from scientific and engineering aspects. However, there are many technical obstacles that impede their practical applications (Fig. 15). From the perspective of practical manufacturing, leady oxide paste and carbon additives need to be mixed homogeneously, which is challenging in that most carbon materials have a low density (< 2.2 g cm^{-3} graphite) compared with lead (11.3 g cm^{-3}) and lead compounds ($PbSO_4$, 6.3 g cm^{-3}; $PbO{\cdot}PbSO_4$, 7.02 g cm^{-3}) [80]. It is necessary to combine lead compounds with carbon additives for the homogeneous distribution of carbon additives in NAMs [121]. Carbon additives should present as slow a hydrogen evolution rate as possible; in that case, their combination with lead seems to be an effective strategy and does not introduce other impurities into NAMs. Therefore, various industrial processes could be developed to manufacture Pb-C composite additives for LCBs. For the preparation of Pb-C composite additives, the homogeneous distribution of Pb on the carbon surface should be taken into account. Oxygen-terminated functional groups can be employed to distribute the Pb species homogeneously. Note that the effectiveness of Pb-C additives should be evaluated by both electrical and physicochemical methodologies. SSA is so important a parameter that it requires more attention. If a large SSA can be retained during the cycling of an LCB, the performance of the Pb negative electrode is not attenuated. The hydrogen evolution rate of an LCB should be evaluated in a real-time charging process by collecting the evolved H_2 gas. Thereby, the dependence of the SoC and the evolution rate of hydrogen gas can be obtained, which can be applied in designing specific charging methods to alleviate hydrogen evolution during

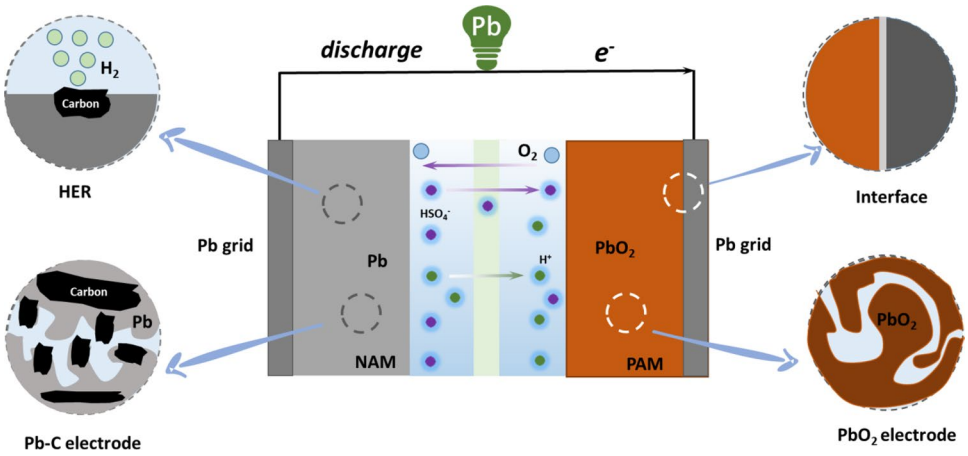

Fig. 15 A summary of the main obstacles and considerations in developing maintenance-free valve-regulated LCBs

charging. Nevertheless, HER is inevitable in the lead-carbon electrode, and as a result, it should be controlled to the minimum that can be accepted by long-term applications. Specifically, the HER rate of the lead-carbon electrode under PSoC conditions should be evaluated because the HER at a low SoC should be lower than that at a high SoC. During a high SoC, the volume of evolved H_2 gas should be collected and analyzed quantitatively. The affinity between lead and carbon needs to be evaluated [114, 115], although it is difficult to evaluate with traditional physicochemical methods. The affinity between lead and carbon determines whether a continuous lead-carbon binary composite interface can be formed. One significant consideration is the approach of using defects to affect the reversible deposition of Pb. Can we establish specific nitrogen doping configurations [181] or oxygen terminated defect sites from a molecular perspective to enhance the reversibility of LCBs? First-principle density function theory methods can be used to determine the active sites for the deposition of Pb. On the one hand, defects may play an important role in enhancing the deposition/dissolution kinetics of lead-carbon electrodes; on the other hand, various defect configurations should be taken into account, namely, oxygen/nitrogen terminated defects, edge sites, nitrogen-replaced graphene sites, and inner vacancy sites. Overall, a high affinity for lead and a low HER rate are conducive to maintaining the robust structure of the Pb-C negative plate, which is essential for long-term cycling.

Although the failure of the PbO_2 positive electrode is not regarded as the major failure mode of LABs operated under PSoC, it still requires PbO_2 to be durable and mechanically robust in an attempt to achieve LCBs with a long cycle life (when deep charge-discharge occurs). Due to the low SoC of PbO_2 under PSoC operation, the corrosion of the positive grid may not be severe; however, the integrity of the PbO_2 particles inside the PAM should be improved to provide a long cycling life. One simple strategy is to employ tubular PbO_2 plates to avoid the shedding of PbO_2 particles. For planar plates, a high-density pasted plate is necessary for the formation process. In addition, it is significant for interface formation between the PAM and the positive grid, which can provide long-lasting performance [182]. In this case, lead-calcium-tin, lead-tin, and other Pb-alloy grids should be applied for valve-regulated LCBs, although lead-antimony shows higher resistance to grid growth. Novel lead-based grids can be designed to increase the robustness of the interface of the positive grid [183]. A novel lead-carbon binary alloy grid may be a favorable choice, and further investigation is required [184]. To design valve-regulated LCBs, the charge between positive and negative electrodes should be balanced with the aim of reducing hydrogen evolution from the design perspective. For O_2 gas combinations, high-speed O_2 diffusion channels are needed, while extra water should be provided by gel electrolytes or aqueous electrolytes in AGMs. The oxidation of O_2 gas toward carbon materials should be evaluated for long-term cycling applications.

7.2 Novel Energy Storage Devices Derived from Lead Acid Batteries (LABs)

LABs are based on the H_2SO_4 electrolyte. Given that the Pb negative electrode does not need protons in the charge-discharge process, acid-free aqueous neutral Li_2SO_4 or Na_2SO_4 electrolytes can be employed in hybrid batteries with spinel $LiMn_2O_4$ positive electrodes and Pb negative electrodes [185]. In a neutral aqueous electrolyte, the corrosion of Pb may be slower, and if so, a long durable Pb negative electrode could be developed. Therefore, various electrochemical energy storage devices could be developed based on Pb negative electrodes that could operate in neutral sulfate electrolytes. Recently, a Mn(II)/MnO_2 positive electrode coupled with a Pb electrode in an acidic H_2SO_4 electrolyte was developed as a high voltage aqueous battery for large-scale energy storage [186]. This battery is based on the deposition of MnO_2 and dissolution of MnO_2 into Mn^{2+} in acidic $MnSO_4$ electrolytes. In acidic electrolytes, Pb can

also be coupled with an organic cathode to construct a Pb-organic battery [187]. The Pb negative electrode can operate in an alkaline electrolyte through transformation between PbO and Pb; in such a way, the Pb/PbO electrode can be coupled with the air electrode to construct a Pb-air battery [188]. Because the PbO_2 positive electrode needs protons in the charge-discharge process, the PbO_2 positive electrode can be coupled with negative electrodes in the acidic H_2SO_4 electrolyte, such as copper deposition/dissolution in H_2SO_4 [189], in such a way that Cu-PbO_2 batteries can be fabricated [190]. If an ion exchange membrane can be employed as the separator, an electrolyte-hybrid battery can be fabricated, and $NiMnH_x$ [191] and zinc anodes [192] operating in alkali KOH electrolyte can be employed as the negative electrode. In this way, a high voltage may be obtained via an electrolyte decoupling strategy. In addition, redox-active polyaniline can be employed as the negative electrode in a hybrid battery based on PbO_2 positive electrodes [193–195]. The conversion mechanism of the PbO_2 positive electrode can also be transformed into a dissolution-deposition mechanism based on the electrodeposition chemistry of PbO_2 film electrodes [21, 62, 63]. One promising configuration is a redox flow LAB based on a methane sulfonic acid electrolyte [185, 196, 197] and a perchlorate electrolyte [198], in which Pb^{2+} ions can be dissolved. In addition, based on the highly stable and mature technologies of Pb and PbO_2 electrodes, LABs can be transformed via chemical engineering tuning of the positive and negative electrode chemistries into various configurations of new battery systems, such as bipolar LABs [199, 200], redox flow batteries [185, 197], batteries with thin film plates [201], and VRLA batteries [44]. In all these systems, a hybrid lead-carbon composite negative electrode can be applied to enhance the electrode kinetics and cycling stability. Is it possible to design a commercial battery based on an LAB system to achieve a higher energy density and a longer cycle life?

7.3 Future Developments and Research Directions of Lead-Carbon Batteries (LCBs)

The LCB is a complicated system that needs a comprehensive design aiming at obtaining a favorable LCB product. We summarize the aspects with respect to future research and development and commercialization activities (Fig. 16). These aspects include active materials, additive engineering, interface engineering, and full cell design. Active materials are the most important components of LCBs, and most research activities are conducted based on the design of durable PAMs and NAMs. For the Pb electrode, the sponge Pb should be highly porous and have a large SSA during repeated cycling. In a lead-carbon hybrid system, the SSA of the NAM can be maintained with carbon additives to decrease the H_2 gassing rate as much as possible. For the PbO_2 electrode, the structure of PbO_2 should be of high density and antisoftening (through the application of tetrabasic lead sulfate high-density paste [157]). Additives play an important role in the evolution of LABs; for carbon additives, carbon materials should be of high density to facilitate the simple incorporation of carbon in the NAM. The pursuit of PAM additives is difficult because PbO_2 is highly oxidative and oxidizes carbon additives [160]. Therefore, various inorganic additives [148, 149, 151] and highly crystalline carbon materials [163] that may avoid oxidation should be developed for

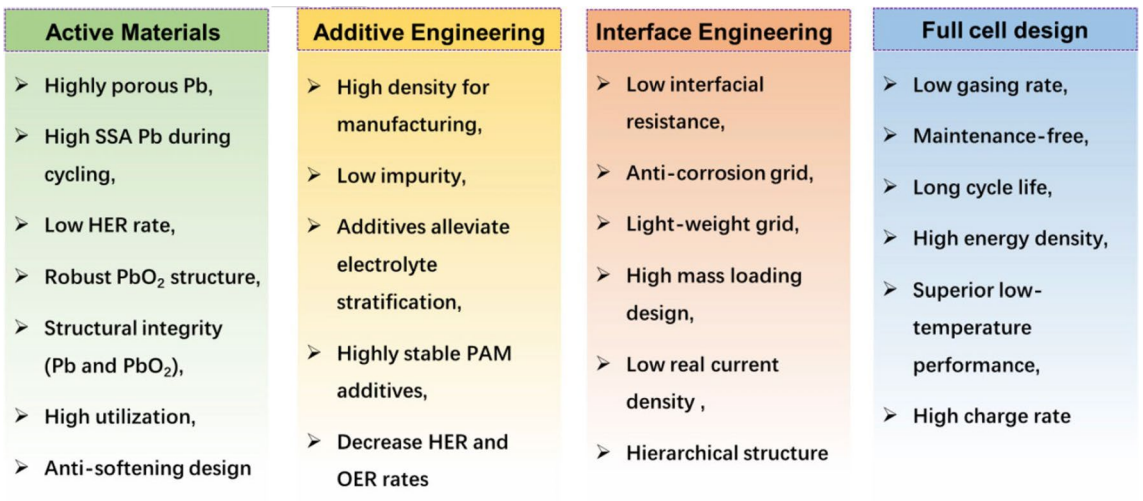

Fig. 16 Comprehensive summaries of the aspects for the future developments of advanced LCBs with engineered strategies of active materials, additive engineering, interface engineering, and full cell design

the commercialization of LCBs. The interfacial phenomenon plays a critical role in the performance of LCBs, which determines the internal resistance and cycling life. The anticorrosive characteristics and mass loading of grid materials should be taken into account during their development in an attempt to enhance the overall specific capacity of NAMs and PAMs. In summary, the ultimate goal of fabricating LCBs should take into account the H_2 gas rate to design maintenance-free LCBs with a long cycling life.

It is clear that the addition of carbon additives in NAMs causes some systemic problems for the design of LCBs; this can be addressed by engineering and scientific strategies. LCBs are undergoing rapid development in research, engineering, and commercialization activities. Therefore, the focus should be placed on aspects such as parasitic reactions, the structural evolution of lead-carbon electrodes during charge-discharge, and the final failure mode of LCBs. LCBs outperform LIBs in renewable energy storage and power management due to their cost-effectiveness, safety, and environmental impacts. With continuous mechanistic studies and technological exploration (interface engineering, additive engineering, active material development, and full cell design), LCBs will be used to obtain a wide range of applications in future energy storage.

Acknowledgements The authors acknowledge the financial support from the National Natural Science Foundation of China (Nos. 22108044, 21573093, 21975101), the Science and Technology Innovation Team Project of Jilin University (No. 2017TD-31), the National Natural Science Foundation of China (No. 21706038), the National Natural Science Foundation of China (No. 22038004), the Natural Science Foundation for Guangdong Province (No. 2019B151502038), the National Key Research and Development Plan (No. 2018YFB1501503), the Research and Development Program in Key Fields of Guangdong Province (2020B1111380002), and the financial support from the Guangdong Provincial Key Laboratory of Plant Resources Biorefinery (2021GDKLPRB07). Wenli Zhang acknowledges the start-up funding of Guangdong University of Technology.

Author's contribution Wenli Zhang, Haibo Lin, and Xueqing Qiu conceived the theme of this article. Wenli Zhang, Haibo Lin, and Jian Yin prepared this article and designed the corresponding schemes and figures. Zheqi Lin, Jun Shi, Yue Wang, and Jinpeng Bao contributed to the writing and modification of this article. Xuliang Lin and Yanlin Qin contributed useful discussions and modifications.

Declarations

Conflict of interest The authors declare no conflicts of interest.

Open Access This article is licensed under a Creative Commons Attribution 4.0 International License, which permits use, sharing, adaptation, distribution and reproduction in any medium or format, as long as you give appropriate credit to the original author(s) and the source, provide a link to the Creative Commons licence, and indicate if changes were made. The images or other third party material in this article are included in the article's Creative Commons licence, unless indicated otherwise in a credit line to the material. If material is not included in the article's Creative Commons licence and your intended use is not permitted by statutory regulation or exceeds the permitted use, you will need to obtain permission directly from the copyright holder. To view a copy of this licence, visit http://creativecommons.org/licenses/by/4.0/.

References

1. Dunn, B., Kamath, H., Tarascon, J.M.: Electrical energy storage for the grid: a battery of choices. Science **334**, 928–935 (2011). https://doi.org/10.1126/science.1212741
2. Yang, Z.G., Zhang, J.L., Kintner-Meyer, M.C.W., et al.: Electrochemical energy storage for green grid. Chem. Rev. **111**, 3577–3613 (2011). https://doi.org/10.1021/cr100290v
3. Moseley, P.T., Rand, D.A.J., Monahov, B.: Designing lead-acid batteries to meet energy and power requirements of future automobiles. J. Power Sour. **219**, 75–79 (2012). https://doi.org/10.1016/j.jpowsour.2012.07.040
4. Soria, M.L., Trinidad, F., Lacadena, J.M., et al.: Advanced valve-regulated lead-acid batteries for hybrid vehicle applications. J. Power Sour. **168**, 12–21 (2007). https://doi.org/10.1016/j.jpowsour.2006.11.086
5. Yin, J., Zhang, W.L., Wang, W.X., et al.: Electrochemical zinc ion capacitors enhanced by redox reactions of porous carbon cathodes. Adv. Energy Mater. **10**, 2001705 (2020). https://doi.org/10.1002/aenm.202001705
6. Zhang, W.L., Lin, H.B., Lu, H.Y., et al.: On the electrochemical origin of the enhanced charge acceptance of the lead-carbon electrode. J. Mater. Chem. A **3**, 4399–4404 (2015). https://doi.org/10.1039/c4ta05891g
7. Pavlov, D.: Invention and development of the lead-acid battery. In: Pavlov, D. (ed.) Lead-Acid Batteries: Science and Technology, pp. 3–32. Elsevier B.V, Amsterdam (2017). https://doi.org/10.1016/B978-0-444-59552-2.00001-8
8. Kurzweil, P.: Gaston planté and his invention of the lead-acid battery: the genesis of the first practical rechargeable battery. J. Power Sour. **195**, 4424–4434 (2010). https://doi.org/10.1016/j.jpowsour.2009.12.126
9. Lopes, P.P., Stamenkovic, V.R.: Past, present, and future of lead-acid batteries. Science **369**, 923–924 (2020). https://doi.org/10.1126/science.abd3352
10. May, G.J., Davidson, A., Monahov, B.: Lead batteries for utility energy storage: a review. J. Energy Storage **15**, 145–157 (2018). https://doi.org/10.1016/j.est.2017.11.008
11. Zhang, W., Yang, J.K., Wu, X., et al.: A critical review on secondary lead recycling technology and its prospect. Renew. Sustain. Energy Rev. **61**, 108–122 (2016). https://doi.org/10.1016/j.rser.2016.03.046
12. Albers, J., Meissner, E., Shirazi, S.: Lead-acid batteries in micro-hybrid vehicles. J. Power Sour. **196**, 3993–4002 (2011). https://doi.org/10.1016/j.jpowsour.2010.11.094
13. Misra, S.S.: Advances in VRLA battery technology for telecommunications. J. Power Sour. **168**, 40–48 (2007). https://doi.org/10.1016/j.jpowsour.2006.11.005
14. Leadbetter, J., Swan, L.G.: Selection of battery technology to support grid-integrated renewable electricity. J. Power Sour. **216**, 376–386 (2012). https://doi.org/10.1016/j.jpowsour.2012.05.081
15. Baldsing, W.G.A., Hamilton, J.A., Hollenkamp, A.F., et al.: Performance of lead/acid batteries in remote-area power-supply applications. J. Power Sour. **35**, 385–394 (1991). https://doi.org/10.1016/0378-7753(91)80056-4
16. Suzuki, K., Nishida, K., Tsubota, M.: Valve-regulated lead/acid batteries for electric vehicles: present and future. J. Power Sour.

59, 171–175 (1996). https://doi.org/10.1016/0378-7753(95)02319-4
17. Garche, J., Moseley, P.T.: Lead-acid batteries for E-bicycles and E-scooters. In: Garche, J., Karden, E., Moseley, P.T., et al. (eds.) Lead-Acid Batteries for Future Automobiles, pp. 527–547. Elsevier B.V., Amsterdam (2017). https://doi.org/10.1016/b978-0-444-63700-0.00018-0
18. Jung, J., Zhang, L., Zhang, J.J.: Lead-acid battery technologies. CRC Press, Boca Raton (2015). https://doi.org/10.1201/b18665
19. Zhou, D.L., Gao, L.J.: Effect of electrochemical preparation methods on structure and properties of PbO_2 anodic layer. Electrochim. Acta **53**, 2060–2064 (2007). https://doi.org/10.1016/j.electacta.2007.09.005
20. Gladstone, J.H., Tribe, A.: The chemistry of the Planté and Faure accumulators. J. Frankl. Inst. **114**, 219–233 (1882). https://doi.org/10.1016/0016-0032(82)90249-6
21. Li, X.H., Pletcher, D., Walsh, F.C.: Electrodeposited lead dioxide coatings. Chem. Soc. Rev. **40**, 3879–3894 (2011). https://doi.org/10.1039/c0cs00213e
22. Ruetschi, P.: Review on the lead-acid battery science and technology. J. Power Sour. **2**, 3–120 (1977). https://doi.org/10.1016/0378-7753(77)85003-9
23. Pavlov, D.: Lead alloys and grids. grid design principles. In: Pavlov, D. (ed.) Lead-Acid Batteries: Science and Technology, pp. 169–243. Elsevier B.V., Amsterdam (2017). https://doi.org/10.1016/b978-0-444-59552-2.00004-3
24. Pavlov, D.: Fundamentals of lead-acid batteries. In: Pavlov, D. (ed.) Lead-Acid Batteries: Science and Technology, pp. 33–129. Elsevier B.V., Amsterdam (2017). https://doi.org/10.1016/b978-0-444-59552-2.00002-x
25. Lam, L.T., Louey, R.: Development of ultra-battery for hybrid-electric vehicle applications. J. Power Sour. **158**, 1140–1148 (2006). https://doi.org/10.1016/j.jpowsour.2006.03.022
26. Pavlov, D.: Lead-carbon electrodes. In: Pavlov, D. (ed.) Lead-Acid Batteries: Science and Technology, pp. 621–662. Elsevier B.V., Amsterdam (2017). https://doi.org/10.1016/b978-0-444-59552-2.00015-8
27. Palacín, M.R., de Guibert, A.: Why do batteries fail? Science **351**, 1253292 (2016). https://doi.org/10.1126/science.1253292
28. Takehara, Z.I.: Dissolution and precipitation reactions of lead sulfate in positive and negative electrodes in lead acid battery. J. Power Sour. **85**, 29–37 (2000). https://doi.org/10.1016/S0378-7753(99)00378-X
29. Shiota, M., Yamaguchi, Y., de Nakayama, Y., et al.: In situ observation of morphology change in lead dioxide surface for lead-acid battery. J. Power Sour. **95**, 203–208 (2001). https://doi.org/10.1016/S0378-7753(00)00644-3
30. Takeuchi, T., Ken, S.W., Tsuboi, Y., et al.: The partial state-of-charge cycle performance of lead-acid batteries. J. Power Sour. **189**, 1190–1198 (2009). https://doi.org/10.1016/j.jpowsour.2009.01.022
31. Yin, J., Lin, Z.Q., Liu, D.B., et al.: Effect of polyvinyl alcohol/nano-carbon colloid on the electrochemical performance of negative plates of lead acid battery. J. Electroanal. Chem. **832**, 152–157 (2019). https://doi.org/10.1016/j.jelechem.2018.10.069
32. Moseley, P.T.: High-rate, valve-regulated lead-acid batteries-suitable for hybrid electric vehicles? J. Power Sour. **84**, 237–242 (1999). https://doi.org/10.1016/S0378-7753(99)00323-7
33. Moseley, P.T.: Consequences of including carbon in the negative plates of valve-regulated lead-acid batteries exposed to high-rate partial-state-of-charge operation. J. Power Sour. **191**, 134–138 (2009). https://doi.org/10.1016/j.jpowsour.2008.08.084
34. Hua, S.N., Zhou, Q.S., Kong, D.L., et al.: Application of valve-regulated lead-acid batteries for storage of solar electricity in stand-alone photovoltaic systems in the northwest areas of China. J. Power Sour. **158**, 1178–1185 (2006). https://doi.org/10.1016/j.jpowsour.2006.02.105
35. Catherino, H.A., Feres, F.F., Trinidad, F.: Sulfation in lead-acid batteries. J. Power Sour. **129**, 113–120 (2004). https://doi.org/10.1016/j.jpowsour.2003.11.003
36. Pavlov, D., Nikolov, P.: Lead-carbon electrode with inhibitor of sulfation for lead-acid batteries operating in the HRPSoC duty. J. Electrochem. Soc. **159**, A1215–A1225 (2012). https://doi.org/10.1149/2.035208jes
37. Soria, M.L., Hernández, J.C., Valenciano, J., et al.: New developments on valve-regulated lead-acid batteries for advanced automotive electrical systems. J. Power Sour. **144**, 473–485 (2005). https://doi.org/10.1016/j.jpowsour.2004.11.005
38. Chang, Y., Mao, X.X., Zhao, Y.F., et al.: Lead-acid battery use in the development of renewable energy systems in China. J. Power Sour. **191**, 176–183 (2009). https://doi.org/10.1016/j.jpowsour.2009.02.030
39. Lam, L.T., Haigh, N.P., Phyland, C.G., et al.: Failure mode of valve-regulated lead-acid batteries under high-rate partial-state-of-charge operation. J. Power Sour. **133**, 126–134 (2004). https://doi.org/10.1016/j.jpowsour.2003.11.048
40. Pavlov, D.: A theory of the grid/positive active-mass (PAM) interface and possible methods to improve PAM utilization and cycle life of lead/acid batteries. J. Power Sour. **53**, 9–21 (1995). https://doi.org/10.1016/0378-7753(94)02152-S
41. Pavlov, D.: The lead-acid battery lead dioxide active mass: a gel-crystal system with proton and electron conductivity. J. Electrochem. Soc. **139**, 3075–3080 (1992). https://doi.org/10.1149/1.2069034
42. Tundorn, P., Chailapakul, O., Tantavichet, N.: Polyaspartate as a gelled electrolyte additive to improve the performance of the gel valve-regulated lead-acid batteries under 100% depth of discharge and partial-state-of charge conditions. J. Solid State Electrochem. **20**, 801–811 (2016). https://doi.org/10.1007/s10008-015-3117-z
43. Czerwiński, A., Wróbel, J., Lach, J., et al.: The charging-discharging behavior of the lead-acid cell with electrodes based on carbon matrix. J. Solid State Electrochem. **22**, 2703–2714 (2018). https://doi.org/10.1007/s10008-018-3981-4
44. Soria, M.L., Trinidad, F., Lacadena, J.M., et al.: Spiral wound valve-regulated lead-acid batteries for hybrid vehicles. J. Power Sour. **174**, 41–48 (2007). https://doi.org/10.1016/j.jpowsour.2007.04.035
45. Yin, J., Zhang, W.L., Alhebshi, N.A., et al.: Synthesis strategies of porous carbon for supercapacitor applications. Small Methods **4**, 1900853 (2020). https://doi.org/10.1002/smtd.201900853
46. Zhang, W.L., Zhang, F., Ming, F.W., et al.: Sodium-ion battery anodes: status and future trends. EnergyChem **1**, 100012 (2019). https://doi.org/10.1016/j.enchem.2019.100012
47. Moseley, P.T., Nelson, R.F., Hollenkamp, A.F.: The role of carbon in valve-regulated lead-acid battery technology. J. Power Sour. **157**, 3–10 (2006). https://doi.org/10.1016/j.jpowsour.2006.02.031
48. Jaiswal, A., Chalasani, S.C.: The role of carbon in the negative plate of the lead-acid battery. J. Energy Storage **1**, 15–21 (2015). https://doi.org/10.1016/j.est.2015.05.002
49. Hu, Y.C., Yang, J.K., Hu, J.P., et al.: Synthesis of nanostructured PbO@C composite derived from spent lead-acid battery for next-generation lead-carbon battery. Adv. Funct. Mater. **28**, 1705294 (2018). https://doi.org/10.1002/adfm.201705294
50. Prengaman, R.D.: Challenges from corrosion-resistant grid alloys in lead acid battery manufacturing. J. Power Sour. **95**, 224–233 (2001). https://doi.org/10.1016/S0378-7753(00)00620-0
51. Laruelle, S., Grugeon-Dewaele, S., Torcheux, L., et al.: The curing reaction study of the active material in the lead-acid battery.

J. Power Sour. **77**, 83–89 (1999). https://doi.org/10.1016/S0378-7753(98)00187-6
52. Lam, L.T., Ozgun, H., Cranswick, L.M.D., et al.: Pulsed-current formation of tetrabasic lead sulfate in cured lead/acid battery plates. J. Power Sour. **42**, 55–70 (1993). https://doi.org/10.1016/0378-7753(93)80137-E
53. Ruetschi, P.: Aging mechanisms and service life of lead-acid batteries. J. Power Sour. **127**, 33–44 (2004). https://doi.org/10.1016/j.jpowsour.2003.09.052
54. Lambert, D.W.H., Manders, J.E., Nelson, R.F., et al.: Strategies for enhancing lead-acid battery production and performance. J. Power Sour. **88**, 130–147 (2000). https://doi.org/10.1016/S0378-7753(99)00521-2
55. Insinga, M.G., Oliveri, R.L., Sunseri, C., et al.: Template electrodeposition and characterization of nanostructured Pb as a negative electrode for lead-acid battery. J. Power Sour. **413**, 107–116 (2019). https://doi.org/10.1016/j.jpowsour.2018.12.033
56. Zhang, W.L., Xu, J.H., Hou, D.X., et al.: Hierarchical porous carbon prepared from biomass through a facile method for supercapacitor applications. J. Colloid Interface Sci. **530**, 338–344 (2018). https://doi.org/10.1016/j.jcis.2018.06.076
57. Kazaryan, S.A., Litvinenko, S.V., Kharisov, G.G.: Self-discharge of heterogeneous electrochemical supercapacitor of $PbO_2|H_2SO_4|C$ related to manganese and titanium ions. J. Electrochem. Soc. **155**, A464 (2008). https://doi.org/10.1149/1.2904456
58. Perret, P., Khani, Z., Brousse, T., et al.: Carbon/PbO_2 asymmetric electrochemical capacitor based on methanesulfonic acid electrolyte. Electrochim. Acta **56**, 8122–8128 (2011). https://doi.org/10.1016/j.electacta.2011.05.125
59. Yu, N.F., Gao, L.J., Zhao, S.H., et al.: Electrodeposited PbO_2 thin film as positive electrode in PbO_2/AC hybrid capacitor. Electrochim. Acta **54**, 3835–3841 (2009). https://doi.org/10.1016/j.electacta.2009.01.086
60. Zhang, W.L., Lin, H.B., Kong, H.S., et al.: High energy density PbO_2/activated carbon asymmetric electrochemical capacitor based on lead dioxide electrode with three-dimensional porous titanium substrate. Int. J. Hydrog. Energy **39**, 17153–17161 (2014). https://doi.org/10.1016/j.ijhydene.2014.08.039
61. Kazaryan, S.A., Kharisov, G.G., Litvinenko, S.V., et al.: Self-discharge related to iron ions and its effect on the parameters of HES $PbO_2|H_2SO_4|C$ systems. J. electrochem. soc. **154**, A751–A759 (2007). https://doi.org/10.1149/1.2775570
62. Zhang, W.L., Lin, H.B., Kong, H.S., et al.: Preparation and characterization of lead dioxide electrode with three-dimensional porous titanium substrate for electrochemical energy storage. Electrochim. Acta **139**, 209–216 (2014). https://doi.org/10.1016/j.electacta.2014.06.175
63. Zhang, W.L., Kong, H.S., Lin, H.B., et al.: Fabrication, characterization and electrocatalytic application of a lead dioxide electrode with porous titanium substrate. J. Alloy. Compd. **650**, 705–711 (2015). https://doi.org/10.1016/j.jallcom.2015.07.222
64. Bao, J.P., Lin, N., Guo, J.X., et al.: Effects of nano-SiO_2 doped PbO_2 as the positive electrode on the performance of lead-carbon hybrid capacitor. J. Colloid Interface Sci. **574**, 377–384 (2020). https://doi.org/10.1016/j.jcis.2020.03.082
65. Bao, J.P., Lin, N., Lin, H.B., et al.: Effect of the lead deposition on the performance of the negative electrode in an aqueous lead-carbon hybrid capacitor. J. Energy Chem. **55**, 509–516 (2021). https://doi.org/10.1016/j.jechem.2020.06.045
66. Nakano, K., Takeshima, S., Furukawa, J.: Technological trends in lead-acid batteries for automotive applications. Furukawa Rev. (2007). https://www.mendeley.com/research/technological-trends-leadacid-batteries-automotive-applications/
67. Lam, L.T., Furukawa, J., Takada, T., et al.: Optimised energy storage devise.US Patent 1,253,1956, 20 Mar 2008
68. Xiang, J.Y., Ding, P., Zhang, H., et al.: Beneficial effects of activated carbon additives on the performance of negative lead-acid battery electrode for high-rate partial-state-of-charge operation. J. Power Sour. **241**, 150–158 (2013). https://doi.org/10.1016/j.jpowsour.2013.04.106
69. Hong, B., Jiang, L.X., Xue, H.T., et al.: Characterization of nano-lead-doped active carbon and its application in lead-acid battery. J. Power Sour. **270**, 332–341 (2014). https://doi.org/10.1016/j.jpowsour.2014.07.145
70. Valenciano, J., Sánchez, A., Trinidad, F., et al.: Graphite and fiberglass additives for improving high-rate partial-state-of-charge cycle life of valve-regulated lead-acid batteries. J. Power Sour. **158**, 851–863 (2006). https://doi.org/10.1016/j.jpowsour.2005.11.058
71. Yang, H., Qiu, Y.B., Guo, X.P.: Effects of PPy, GO and PPy/GO composites on the negative plate and on the high-rate partial-state-of-charge performance of lead-acid batteries. Electrochim. Acta **215**, 346–356 (2016). https://doi.org/10.1016/j.electacta.2016.08.115
72. Shapira, R., Nessim, G.D., Zimrin, T., et al.: Towards promising electrochemical technology for load leveling applications: extending cycle life of lead acid batteries by the use of carbon nano-tubes (CNTs). Energy Environ. Sci. **6**, 587–594 (2013). https://doi.org/10.1039/c2ee22970f
73. Blecua, M., Fatas, E., Ocon, P., et al.: Graphitized carbon nanofibers: new additive for the negative active material of lead acid batteries. Electrochim. Acta **257**, 109–117 (2017). https://doi.org/10.1016/j.electacta.2017.10.067
74. Xiang, J.Y., Hu, C., Chen, L.Y., et al.: Enhanced performance of Zn(II)-doped lead-acid batteries with electrochemical active carbon in negative mass. J. Power Sour. **328**, 8–14 (2016). https://doi.org/10.1016/j.jpowsour.2016.07.113
75. Zhao, L., Chen, B.S., Wu, J.Z., et al.: Study of electrochemically active carbon, Ga_2O_3 and Bi_2O_3 as negative additives for valve-regulated lead-acid batteries working under high-rate, partial-state-of-charge conditions. J. Power Sour. **248**, 1–5 (2014). https://doi.org/10.1016/j.jpowsour.2013.09.056
76. Lian, J.L., Li, W., Wang, F., et al.: Enhanced performance of lead acid batteries with $Bi_2O_2CO_3$/activated carbon additives to negative plates. J. Electrochem. Soc. **164**, A1726–A1730 (2017). https://doi.org/10.1149/2.1561707jes
77. Zhao, L., Chen, B.S., Wang, D.L.: Effects of electrochemically active carbon and indium (III) oxide in negative plates on cycle performance of valve-regulated lead-acid batteries during high-rate partial-state-of-charge operation. J. Power Sour. **231**, 34–38 (2013). https://doi.org/10.1016/j.jpowsour.2012.12.083
78. Wang, J.X., Hou, H.J., Hu, J.P., et al.: Mechano-chemical synthesis of high-stable PbO@C composite for enhanced performance of lead-carbon battery. Electrochim. Acta **299**, 682–691 (2019). https://doi.org/10.1016/j.electacta.2019.01.063
79. Pavlov, D.: Processes during formation of negative battery plates. In: Pavlov, D. (ed.) Lead-Acid Batteries: Science and Technology, pp. 501–519. Elsevier B.V., Amsterdam (2017). https://doi.org/10.1016/b978-0-444-59552-2.00011-0
80. Liu, Y., Gao, P.R., Bu, X.F., et al.: Nanocrosses of lead sulphate as the negative active material of lead acid batteries. J. Power Sour. **263**, 1–6 (2014). https://doi.org/10.1016/j.jpowsour.2014.03.135
81. Pavlov, D.: Additives to the pastes for positive and negative battery plates. In: Pavlov, D. (ed.) Lead-Acid Batteries: Science and Technology, pp. 335–379. Elsevier B.V., Amsterdam (2017). https://doi.org/10.1016/b978-0-444-59552-2.00007-9
82. Iliev, V., Pavlov, D.: The effect of the expander upon the two types of negative active mass structure in lead-acid batteries. J. Appl. Electrochem. **15**, 39–52 (1985). https://doi.org/10.1007/BF00617739

83. Matrakova, M., Rogachev, T., Pavlov, D., et al.: Influence of phenolic group content in lignin expanders on the performance of negative lead-acid battery plates. J. Power Sour. **113**, 345–354 (2003). https://doi.org/10.1016/S0378-7753(02)00547-5
84. Hirai, N., Tanaka, T., Kubo, S., et al.: Fundamental study of effect of quinone structures in the lignin preparations on negative electrode of lead-acid battery. J. Power Sour. **158**, 846–850 (2006). https://doi.org/10.1016/j.jpowsour.2005.11.010
85. Hirai, N., Tabayashi, D., Shiota, M., et al.: In situ electrochemical atomic force microscopy of lead electrodes in sulfuric acid solution with or without lignin during anodic oxidation and cathodic reduction. J. Power Sour. **133**, 32–38 (2004). https://doi.org/10.1016/j.jpowsour.2003.12.020
86. Boden, D.P.: Comparison of methods for adding expander to lead-acid battery plates-advantages and disadvantages. J. Power Sour. **133**, 47–51 (2004). https://doi.org/10.1016/j.jpowsour.2003.12.006
87. Hirai, N., Tanaka, T., Kubo, S., et al.: Density and hardness of negative pastes of lead-acid batteries containing organic additives with or without quinone structure. J. Power Sour. **158**, 1106–1109 (2006). https://doi.org/10.1016/j.jpowsour.2006.02.002
88. Ken, S.W., Funato, T., Watanabe, M., et al.: Development of additives in negative active-material to suppress sulfation during high-rate partial-state-of-charge operation of lead-acid batteries. J. Power Sour. **158**, 1084–1090 (2006). https://doi.org/10.1016/j.jpowsour.2006.01.096
89. Pavlov, D., Nikolov, P., Rogachev, T.: Influence of expander components on the processes at the negative plates of lead-acid cells on high-rate partial-state-of-charge cycling. Part II. Effect of carbon additives on the processes of charge and discharge of negative plates. J. Power Sour. **195**, 4444–4457 (2010). https://doi.org/10.1016/j.jpowsour.2009.12.132
90. Vermesan, H., Hirai, N., Shiota, M., et al.: Effect of barium sulfate and strontium sulfate on charging and discharging of the negative electrode in a lead-acid battery. J. Power Sour. **133**, 52–58 (2004). https://doi.org/10.1016/j.jpowsour.2003.11.071
91. de Nakayama, Y., Hojo, E., Koike, T.: Development of VRLA battery for hybrid bus. J. Power Sour. **124**, 551–558 (2003). https://doi.org/10.1016/S0378-7753(03)00742-0
92. Fernández, M., Valenciano, J., Trinidad, F., et al.: The use of activated carbon and graphite for the development of lead-acid batteries for hybrid vehicle applications. J. Power Sour. **195**, 4458–4469 (2010). https://doi.org/10.1016/j.jpowsour.2009.12.131
93. Pavlov, D., Rogachev, T., Nikolov, P., et al.: Mechanism of action of electrochemically active carbons on the processes that take place at the negative plates of lead-acid batteries. J. Power Sour. **191**, 58–75 (2009). https://doi.org/10.1016/j.jpowsour.2008.11.056
94. Pavlov, D., Nikolov, P., Rogachev, T.: Influence of carbons on the structure of the negative active material of lead-acid batteries and on battery performance. J. Power Sour. **196**, 5155–5167 (2011). https://doi.org/10.1016/j.jpowsour.2011.02.014
95. Endo, M., Kim, Y.A., Hayashi, T., et al.: Vapor-grown carbon fibers (VGCFs): basic properties and their battery applications. Carbon **39**, 1287–1297 (2001). https://doi.org/10.1016/S0008-6223(00)00295-5
96. Boden, D.P., Loosemore, D.V., Spence, M.A., et al.: Optimization studies of carbon additives to negative active material for the purpose of extending the life of VRLA batteries in high-rate partial-state-of-charge operation. J. Power Sour. **195**, 4470–4493 (2010). https://doi.org/10.1016/j.jpowsour.2009.12.069
97. Ebner, E., Burow, D., Panke, J., et al.: Carbon blacks for lead-acid batteries in micro-hybrid applications: studied by transmission electron microscopy and Raman spectroscopy. J. Power Sour. **222**, 554–560 (2013). https://doi.org/10.1016/j.jpowsour.2012.08.089
98. Shiomi, M., Funato, T., Nakamura, K., et al.: Effects of carbon in negative plates on cycle-life performance of valve-regulated lead/acid batteries. J. Power Sour. **64**, 147–152 (1997). https://doi.org/10.1016/S0378-7753(96)02515-3
99. Kozawa, A., Oho, H., Sano, M., et al.: Beneficial effect of carbon-PVA colloid additives for lead-acid batteries. J. Power Sour. **80**, 12–16 (1999). https://doi.org/10.1016/S0378-7753(99)00162-7
100. Swogger, S.W., Everill, P., Dubey, D.P., et al.: Discrete carbon nanotubes increase lead acid battery charge acceptance and performance. J. Power Sour. **261**, 55–63 (2014). https://doi.org/10.1016/j.jpowsour.2014.03.049
101. Saravanan, M., Sennu, P., Ganesan, M., et al.: Multi-walled carbon nanotubes percolation network enhanced the performance of negative electrode for lead-acid battery. J. Electrochem. Soc. **160**, A70–A76 (2012). https://doi.org/10.1149/2.062301jes
102. Marom, R., Ziv, B., Banerjee, A., et al.: Enhanced performance of starter lighting ignition type lead-acid batteries with carbon nanotubes as an additive to the active mass. J. Power Sour. **296**, 78–85 (2015). https://doi.org/10.1016/j.jpowsour.2015.07.007
103. Mithin Kumar, S., Arun, S., Mayavan, S.: Effect of carbon nanotubes with varying dimensions and properties on the performance of lead acid batteries operating under high rate partial state of charge conditions. J. Energy Storage **24**, 100806 (2019). https://doi.org/10.1016/j.est.2019.100806
104. Yang, H., Qi, K., Gong, L.Q., et al.: Lead oxide enveloped in N-doped graphene oxide composites for enhanced high-rate partial-state-of-charge performance of lead-acid battery. ACS Sustain. Chem. Eng. **6**, 11408–11413 (2018). https://doi.org/10.1021/acssuschemeng.8b01357
105. Naresh, V., Bhattacharjee, U., Martha, S.K.: Boron doped graphene nanosheets as negative electrode additive for high-performance lead-acid batteries and ultracapacitors. J. Alloy Compd. **797**, 595–605 (2019). https://doi.org/10.1016/j.jallcom.2019.04.311
106. Li, X.L., Zhang, Y.Y., Su, Z.L., et al.: Graphene nanosheets as backbones to build a 3D conductive network for negative active materials of lead-acid batteries. J. Appl. Electrochem. **47**, 619–630 (2017). https://doi.org/10.1007/s10800-017-1067-0
107. Yeung, K.K., Zhang, X.F., Kwok, S.C.T., et al.: Enhanced cycle life of lead-acid battery using graphene as a sulfation suppression additive in negative active material. RSC Adv. **5**, 71314–71321 (2015). https://doi.org/10.1039/c5ra11114e
108. Yin, J., Lin, N., Lin, Z.Q., et al.: Hierarchical porous carbon@PbO_{1-x} composite for high-performance lead-carbon battery towards renewable energy storage. Energy **193**, 116675 (2020). https://doi.org/10.1016/j.energy.2019.116675
109. Lin, Z.Q., Lin, N., Lin, H.B., et al.: Significance of PbO deposition ratio in activated carbon-based lead-carbon composites for lead-carbon battery under high-rate partial-state-of-charge operation. Electrochim. Acta **338**, 135868 (2020). https://doi.org/10.1016/j.electacta.2020.135868
110. Lin, Z.Q., Zhang, W.L., Lin, N., et al.: Long-life lead-acid battery for high-rate partial-state-of-charge operation enabled by a rice-husk-based activated carbon negative electrode additive. ChemistrySelect **5**, 2551–2558 (2020). https://doi.org/10.1002/slct.201904280
111. Micka, K., Calábek, M., Bača, P., et al.: Studies of doped negative valve-regulated lead-acid battery electrodes. J. Power Sour. **191**, 154–158 (2009). https://doi.org/10.1016/j.jpowsour.2009.01.014
112. Křivík, P., Micka, K., Bača, P., et al.: Effect of additives on the performance of negative lead-acid battery electrodes during formation and partial state of charge operation. J. Power Sour.

209, 15–19 (2012). https://doi.org/10.1016/j.jpowsour.2011.11.058
113. Zhang, W.L., Yin, J., Lin, Z.Q., et al.: Lead-carbon electrode designed for renewable energy storage with superior performance in partial state of charge operation. J. Power Sour. **342**, 183–191 (2017). https://doi.org/10.1016/j.jpowsour.2016.12.061
114. Settelein, J., Lorrmann, H., Sextl, G.: Evaluating the lead affinity of graphite additives in lead-acid batteries by electrochemical deposition. Electrochim. Acta **233**, 173–180 (2017). https://doi.org/10.1016/j.electacta.2017.03.034
115. Cericola, D., Spahr, M.: Nucleation and electrolytic deposition of lead on model carbon electrodes. J. Power Sour. **324**, 41–44 (2016). https://doi.org/10.1016/j.jpowsour.2016.05.046
116. Settelein, J., Oehm, J., Bozkaya, B., et al.: The external surface area of carbon additives as key to enhance the dynamic charge acceptance of lead-carbon electrodes. J. Energy Storage **15**, 196–204 (2018). https://doi.org/10.1016/j.est.2017.11.016
117. Monahov, B.: The beneficial role of carbon in the negative plate of advanced lead-carbon batteries. ECS Trans. **41**, 45–69 (2019). https://doi.org/10.1149/1.3691910
118. Wang, F., Hu, C., Zhou, M., et al.: Research progresses of cathodic hydrogen evolution in advanced lead-acid batteries. Sci. Bull. **61**, 451–458 (2016). https://doi.org/10.1007/s11434-016-1023-0
119. Peters, K., Rand, D.A.J., Moseley, P.T.: performance-enhancing materials for lead-acid battery negative plates. In: Peters, K., Rand, D.A.J., Moseley, P.T. (eds.) Lead-Acid Batteries for Future Automobiles, pp. 213–234. Elsevier BV, Amsterdam (2017). https://doi.org/10.1016/b978-0-444-63700-0.00007-6
120. Ebner, E., Burow, D., Börger, A., et al.: Carbon blacks for the extension of the cycle life in flooded lead acid batteries for micro-hybrid applications. J. Power Sour. **239**, 483–489 (2013). https://doi.org/10.1016/j.jpowsour.2013.03.124
121. Fan, N., Li, X.H., Li, H., et al.: The application of spray drying method in valve-regulated lead-acid battery. J. Power Sour. **223**, 114–118 (2013). https://doi.org/10.1016/j.jpowsour.2012.09.041
122. Zou, X.P., Kang, Z.X., Shu, D., et al.: Effects of carbon additives on the performance of negative electrode of lead-carbon battery. Electrochim. Acta **151**, 89–98 (2015). https://doi.org/10.1016/j.electacta.2014.11.027
123. Yin, J., Lin, N., Lin, Z.Q., et al.: Towards renewable energy storage: understanding the roles of rice husk-based hierarchical porous carbon in the negative electrode of lead-carbon battery. J. Energy Storage **24**, 100756 (2019). https://doi.org/10.1016/j.est.2019.100756
124. Enos, D.G., Ferreira, S.R., Barkholtz, H.M., et al.: Understanding function and performance of carbon additives in lead-acid batteries. J. Electrochem. Soc. **164**, A3276–A3284 (2017). https://doi.org/10.1149/2.1031713jes
125. Conway, B.E., Bockris, J.O.: Electrolytic hydrogen evolution kinetics and its relation to the electronic and adsorptive properties of the metal. J. Chem. Phys. **26**, 532–541 (1957). https://doi.org/10.1063/1.1743339
126. Kamenev, Y.B., Kiselevich, A.V., Ostapenko, E.I., et al.: Effect of benzaldehyde derivatives on the rate of hydrogen evolution in a sealed lead-acid battery. Russ. J. Appl. Chem. **77**, 1455–1459 (2004). https://doi.org/10.1007/s11167-005-0052-2
127. Deyab, M.A.: Ionic liquid as an electrolyte additive for high performance lead-acid batteries. J. Power Sour. **390**, 176–180 (2018). https://doi.org/10.1016/j.jpowsour.2018.04.053
128. Deyab, M.A.: Hydrogen evolution inhibition by l-serine at the negative electrode of a lead-acid battery. RSC Adv. **5**, 41365–41371 (2015). https://doi.org/10.1039/c5ra05044h
129. Wu, Z.F., Liu, Y., Deng, C.Z., et al.: The critical role of boric acid as electrolyte additive on the electrochemical performance of lead-acid battery. J. Energy Storage **27**, 101076 (2020). https://doi.org/10.1016/j.est.2019.101076
130. Wang, L.Y., Zhang, H., Cao, G.P., et al.: Effect of activated carbon surface functional groups on nano-lead electrodeposition and hydrogen evolution and its applications in lead-carbon batteries. Electrochim. Acta **186**, 654–663 (2015). https://doi.org/10.1016/j.electacta.2015.11.007
131. Wang, H., Liu, Z., Liang, Q.Q., et al.: A facile method for preparation of doped-N carbon material based on sisal and application for lead-carbon battery. J. Clean. Prod. **197**, 332–338 (2018). https://doi.org/10.1016/j.jclepro.2018.06.214
132. Wang, F., Hu, C., Lian, J.L., et al.: Phosphorus-doped activated carbon as a promising additive for high performance lead carbon batteries. RSC Adv. **7**, 4174–4178 (2017). https://doi.org/10.1039/c6ra26093d
133. Tong, P.Y., Zhao, R.R., Zhang, R.B., et al.: Characterization of lead (II)-containing activated carbon and its excellent performance of extending lead-acid battery cycle life for high-rate partial-state-of-charge operation. J. Power Sour. **286**, 91–102 (2015). https://doi.org/10.1016/j.jpowsour.2015.03.150
134. Yin, J., Lin, N., Lin, Z.Q., et al.: Optimized lead carbon composite for enhancing the performance of lead-carbon battery under HRPSoC operation. J. Electroanal. Chem. **832**, 266–274 (2019). https://doi.org/10.1016/j.jelechem.2018.10.022
135. Zhang, S.K., Zhang, H., Xue, W.H., et al.: A layered-carbon/$PbSO_4$ composite as a new additive for negative active material of lead-acid batteries. Electrochim. Acta **290**, 46–54 (2018). https://doi.org/10.1016/j.electacta.2018.08.090
136. Wang, L.Y., Zhang, W.F., Gu, L., et al.: Tracking the morphology evolution of nano-lead electrodeposits on the internal surface of porous carbon and its influence on lead-carbon batteries. Electrochim. Acta **222**, 376–384 (2016). https://doi.org/10.1016/j.electacta.2016.10.189
137. Moncada, A., Mistretta, M.C., Randazzo, S., et al.: High-performance of PbO_2 nanowire electrodes for lead-acid battery. J. Power Sour. **256**, 72–79 (2014). https://doi.org/10.1016/j.jpowsour.2014.01.050
138. Egan, D.R.P., Low, C.T.J., Walsh, F.C.: Electrodeposited nanostructured lead dioxide as a thin film electrode for a lightweight lead-acid battery. J. Power Sour. **196**, 5725–5730 (2011). https://doi.org/10.1016/j.jpowsour.2011.01.008
139. Pavlov, D., Balkanov, I.: The PbO_2 particle: exchange reactions between ions of the electrolyte and the PbO_2 particles of the lead-acid battery positive active mass. J. Electrochem. Soc. **139**, 1830–1835 (1992). https://doi.org/10.1149/1.2069506
140. Pavlov, D., Balkanov, I., Halachev, T., et al.: Hydration and amorphization of active mass PbO_2 particles and their influence on the electrical properties of the lead-acid battery positive plate. J. Electrochem. Soc. **136**, 3189–3197 (1989). https://doi.org/10.1149/1.2096424
141. Fitas, R., Zerroual, L., Chelali, N., et al.: Thermal degradation of α- and β-PbO_2 and its relationship to capacity loss. J. Power Sour. **85**, 56–58 (2000). https://doi.org/10.1016/S0378-7753(99)00382-1
142. Zerroual, L., Fitas, R., Djellouli, B., et al.: Relationship between water departure and capacity loss of α and β-PbO_2 using an all solid-state system: estimation of proton diffusion coefficient. J. Power Sour. **158**, 837–840 (2006). https://doi.org/10.1016/j.jpowsour.2005.11.011
143. Fan, N., Sun, C.H., Kong, D.L., et al.: Chemical synthesis of PbO_2 particles with multiple morphologies and phases and their electrochemical performance as the positive active material. J. Power Sour. **254**, 323–328 (2014). https://doi.org/10.1016/j.jpowsour.2013.12.077
144. Ding, L.X., Zheng, F.L., Wang, J.W., et al.: Super-large dendrites composed of trigonal PbO_2 nanoplates with enhanced

performances for electrochemical devices. Chem. Commun. **48**, 1275–1277 (2012). https://doi.org/10.1039/c2cc15271a
145. Chen, T., Huang, H., Ma, H.Y., et al.: Effects of surface morphology of nanostructured PbO_2 thin films on their electrochemical properties. Electrochim. Acta **88**, 79–85 (2013). https://doi.org/10.1016/j.electacta.2012.10.009
146. Bashtavelova, E., Winsel, A.: Paste structure and its influence on the agglomerate-of-spheres parameters of the PbO_2 electrode. J. Power Sour. **53**, 175–183 (1995). https://doi.org/10.1016/0378-7753(94)01985-5
147. Shi, J., Lin, N., Wang, Y., et al.: The application of rice husk-based porous carbon in positive electrodes of lead acid batteries. J. Energy Storage **30**, 101392 (2020). https://doi.org/10.1016/j.est.2020.101392
148. Foudia, M., Matrakova, M., Zerroual, L.: Effect of a mineral additive on the electrical performances of the positive plate of lead acid battery. J. Power Sour. **279**, 146–150 (2015). https://doi.org/10.1016/j.jpowsour.2015.01.008
149. Sorge, M., Bean, T., Woodland, T., et al.: Investigating the use of porous, hollow glass microspheres in positive lead acid battery plates. J. Power Sour. **266**, 496–511 (2014). https://doi.org/10.1016/j.jpowsour.2014.05.021
150. Ponraj, R., McAllister, S.D., Cheng, I.F., et al.: Investigation on electronically conductive additives to improve positive active material utilization in lead-acid batteries. J. Power Sour. **189**, 1199–1203 (2009). https://doi.org/10.1016/j.jpowsour.2008.12.077
151. Newell, J.D., Patankar, S.N., Edwards, D.B.: Porous microspheres as additives in lead-acid batteries. J. Power Sour. **188**, 292–295 (2009). https://doi.org/10.1016/j.jpowsour.2008.11.067
152. Naresh, V., Elias, L., Gaffoor, S.A., et al.: Corrosion resistant polypyrrole coated lead-alloy positive grids for advanced lead-acid batteries. J. Electrochem. Soc. **166**, A74–A81 (2019). https://doi.org/10.1149/2.0211902jes
153. Yang, B.F., Cai, X.Y., Li, E.Y., et al.: Evaluation of the effect of additive group five elements on the properties of Pb-Ca-Sn-Al alloy as the positive grid for lead-acid batteries. J. Solid State Electrochem. **23**, 1715–1725 (2019). https://doi.org/10.1007/s10008-019-04265-x
154. Lannelongue, J., Cugnet, M., Guillet, N., et al.: Operation of thin-plate positive lead-acid battery electrodes employing titanium current collectors. J. Energy Storage **20**, 230–243 (2018). https://doi.org/10.1016/j.est.2018.09.020
155. Kong, H.S., Huang, W.M., Lin, H.B., et al.: Effect of SnO_2-Sb_2O_5 interlayer on electrochemical performances of a Ti-substrate lead dioxide electrode. Chin. J. Chem. **30**, 2059–2065 (2012). https://doi.org/10.1002/cjoc.201200627
156. Pavlov, D., Kapkov, N.: Lead-acid battery pastes containing $4PbO{\cdot}PbSO_4$ and Pb_3O_4. J. Electrochem. Soc. **137**, 16–21 (1990). https://doi.org/10.1149/1.2086354
157. Lang, X.S., Wang, D.L., Hu, C.Y., et al.: The use of nanometer tetrabasic lead sulfate as positive active material additive for valve regulated lead-acid battery. J. Power Sour. **270**, 9–13 (2014). https://doi.org/10.1016/j.jpowsour.2014.07.101
158. Zhang, K., Liu, W., Ma, B.B., et al.: Lead sulfate used as the positive active material of lead acid batteries. J. Solid State Electrochem. **20**, 2267–2273 (2016). https://doi.org/10.1007/s10008-016-3243-2
159. Dietz, H., Garche, J., Wiesener, K.: The effect of additives on the positive lead-acid battery electrode. J. Power Sour. **14**, 305–319 (1985). https://doi.org/10.1016/0378-7753(85)80046-X
160. Dietz, H., Garche, J., Wiesener, K.: On the behaviour of carbon black in positive lead-acid battery electrodes. J. Appl. Electrochem. **17**, 473–479 (1987). https://doi.org/10.1007/BF01084120
161. Chahmana, N., Zerroual, L., Matrakova, M.: Influence of Mg^{2+}, Al^{3+}, Co^{2+}, Sn^{2+} and Sb^{3+} on the electrical performance of doped β-lead dioxide. J. Power Sour. **191**, 144–148 (2009). https://doi.org/10.1016/j.jpowsour.2008.10.115
162. Moncada, A., Piazza, S., Sunseri, C., et al.: Recent improvements in PbO_2 nanowire electrodes for lead-acid battery. J. Power Sour. **275**, 181–188 (2015). https://doi.org/10.1016/j.jpowsour.2014.10.189
163. Banerjee, A., Ziv, B., Shilina, Y., et al.: Single-wall carbon nanotube doping in lead-acid batteries: a new horizon. ACS Appl. Mater. Interfaces **9**, 3634–3643 (2017). https://doi.org/10.1021/acsami.6b13377
164. Pavlov, D.: Valve-regulated lead-acid (VRLA) batteries. In: Pavlov, D. (ed.) Lead-Acid Batteries: Science and Technology, pp. 593–620. Elsevier B.V., Amsterdam (2017). https://doi.org/10.1016/b978-0-444-59552-2.00014-6
165. Büngeler, J., Cattaneo, E., Riegel, B., et al.: Advantages in energy efficiency of flooded lead-acid batteries when using partial state of charge operation. J. Power Sour. **375**, 53–58 (2018). https://doi.org/10.1016/j.jpowsour.2017.11.050
166. Hammouche, A., Thele, M., Sauer, D.U.: Analysis of gassing processes in a VRLA/spiral wound battery. J. Power Sour. **158**, 987–990 (2006). https://doi.org/10.1016/j.jpowsour.2005.11.046
167. Pavlov, D., Papazov, G., Monahov, B.: Strap grid tubular plate: a new positive plate for lead-acid batteries: processes of residual sulphation of the positive plate. J. Power Sour. **113**, 255–270 (2003). https://doi.org/10.1016/S0378-7753(02)00521-9
168. Bullock, K.R.: Carbon reactions and effects on valve-regulated lead-acid (VRLA) battery cycle life in high-rate, partial state-of-charge cycling. J. Power Sour. **195**, 4513–4519 (2010). https://doi.org/10.1016/j.jpowsour.2009.10.027
169. Lambert, D.W.H., Greenwood, P.H.J., Reed, M.C.: Advances in gelled-electrolyte technology for valve-regulated lead-acid batteries. J. Power Sour. **107**, 173–179 (2002). https://doi.org/10.1016/S0378-7753(01)01072-2
170. Rand, D.A.J.: Energy storage with lead-acid batteries. In: Rand, D.A.J., Moseley, P.T. (eds.) Electrochemical Energy Storage for Renewable Sources and Grid Balancing, pp. 201–222. Elsevier B.V., Amsterdam (2015). https://doi.org/10.1016/b978-0-444-62616-5.00013-9
171. Li, H., Liu, H.P., Wang, Q.M., et al.: Effects of covalently bonded siloxane on the electrochemical and physical behaviour of GEL-VRLA battery. Electrochim. Acta **56**, 663–666 (2010). https://doi.org/10.1016/j.electacta.2010.09.075
172. Wu, L., Chen, H.Y., Jiang, X.: Effect of silica soot on behaviour of negative electrode in lead-acid batteries. J. Power Sour. **107**, 162–166 (2002). https://doi.org/10.1016/S0378-7753(01)01001-1
173. Gençten, M., Dönmez, K.B., Şahin, Y., et al.: Voltammetric and electrochemical impedimetric behavior of silica-based gel electrolyte for valve-regulated lead-acid battery. J. Solid State Electrochem. **18**, 2469–2479 (2014). https://doi.org/10.1007/s10008-014-2507-y
174. Tuphorn, H.: Gelled-electrolyte batteries for electric vehicles. J. Power Sour. **40**, 47–61 (1992). https://doi.org/10.1016/0378-7753(92)80037-C
175. Tang, Z., Wang, J.M., Mao, X.X., et al.: Investigation and application of polysiloxane-based gel electrolyte in valve-regulated lead-acid battery. J. Power Sour. **168**, 49–57 (2007). https://doi.org/10.1016/j.jpowsour.2006.12.031
176. Dimitrov, M., Pavlov, D., Rogachev, T., et al.: Processes taking place in the paste of lead-acid battery plates during soaking prior to formation and their influence on battery performance. J. Power

Sour. **140**, 168–180 (2005). https://doi.org/10.1016/j.jpowsour.2004.08.006
177. Isoi, T., Furukawa, H.: Valve-regulated lead/acid batteries for SLI use in Japan. J. Power Sour. **59**, 143–146 (1996). https://doi.org/10.1016/0378-7753(95)02315-1
178. Ball, R.J., Kurian, R., Evans, R., et al.: Failure mechanisms in valve regulated lead/acid batteries for cyclic applications. J. Power Sour. **109**, 189–202 (2002). https://doi.org/10.1016/S0378-7753(02)00071-X
179. Valenciano, J., Fernández, M., Trinidad, F., et al.: Lead-acid batteries for micro- and mild-hybrid applications. J. Power Sour. **187**, 599–604 (2009). https://doi.org/10.1016/j.jpowsour.2008.11.089
180. Subburaj, A.S., Pushpakaran, B.N., Bayne, S.B.: Overview of grid connected renewable energy based battery projects in USA. Renew. Sustain. Energy Rev. **45**, 219–234 (2015). https://doi.org/10.1016/j.rser.2015.01.052
181. Zhang, W.L., Sun, M.L., Yin, J., et al.: A cyclized polyacrylonitrile anode for alkali metal ion batteries. Angew. Chem. Int. Edit. **60**, 1355–1363 (2021). https://doi.org/10.1002/anie.202011484
182. Meyers, J.P., de Guzman, R.C., Swogger, S.W., et al.: Discrete carbon nanotubes promote resistance to corrosion in lead-acid batteries by altering the grid-active material interface. J. Energy Storage **32**, 101983 (2020). https://doi.org/10.1016/j.est.2020.101983
183. Zhang, S.K., Zhang, H., Cheng, J., et al.: Novel polymer-graphite composite grid as a negative current collector for lead-acid batteries. J. Power Sour. **334**, 31–38 (2016). https://doi.org/10.1016/j.jpowsour.2016.09.097
184. Yolshina, L.A., Yolshina, V.A., Yolshin, A.N., et al.: Novel lead-graphene and lead-graphite metallic composite materials for possible applications as positive electrode grid in lead-acid battery. J. Power Sour. **278**, 87–97 (2015). https://doi.org/10.1016/j.jpowsour.2014.12.036
185. Zhang, C.P., Sharkh, S.M., Li, X., et al.: The performance of a soluble lead-acid flow battery and its comparison to a static lead-acid battery. Energy Convers. Manag. **52**, 3391–3398 (2011). https://doi.org/10.1016/j.enconman.2011.07.006
186. Huang, J.H., Yan, L., Bin, D., et al.: An aqueous manganese-lead battery for large-scale energy storage. J. Mater. Chem. A **8**, 5959–5967 (2020). https://doi.org/10.1039/d0ta01484b
187. Yue, F., Tie, Z.W., Deng, S.Z., et al.: An ultralow temperature aqueous battery with proton chemistry. Angew. Chem. Int. Edit **60**, 13882–13886 (2021). https://doi.org/10.1002/anie.202103722
188. Wang, P.Y., Pan, J.Q., Gong, S.M., et al.: A green preparation method of battery grade α-PbO based on Pb-O_2 fuel cell. J. Power Sour. **360**, 324–327 (2017). https://doi.org/10.1016/j.jpowsour.2017.05.107
189. Liang, G., Mo, F., Yang, Q., et al.: Commencing an acidic battery based on a copper anode with ultrafast proton-regulated kinetics and superior dendrite-free property. Adv. Mater. **31**, 1905873 (2019). https://doi.org/10.1002/adma.201905873
190. Pan, J.Q., Sun, Y.Z., Cheng, J., et al.: Study on a new single flow acid Cu-PbO_2 battery. Electrochem. Commun. **10**, 1226–1229 (2008). https://doi.org/10.1016/j.elecom.2008.06.008
191. Li, H.Q., Weng, G.M., Li, C.Y.V., et al.: Three electrolyte high voltage acid-alkaline hybrid rechargeable battery. Electrochim. Acta **56**, 9420–9425 (2011). https://doi.org/10.1016/j.electacta.2011.08.027
192. Xu, Y.P., Cai, P.W., Chen, K., et al.: High-voltage rechargeable alkali-acid Zn-PbO_2 hybrid battery. Angew. Chem. Int. Edit **59**, 23593–23597 (2020). https://doi.org/10.1002/anie.202012017
193. Grgur, B.N., Ristić, V., Gvozdenović, M.M., et al.: Polyaniline as possible anode materials for the lead acid batteries. J. Power Sour. **180**, 635–640 (2008). https://doi.org/10.1016/j.jpowsour.2008.02.022
194. Martha, S.K., Hariprakash, B., Gaffoor, S.A., et al.: Lead-acid cells with polyaniline-coated negative plates. J. Appl. Electrochem. **36**, 711–722 (2006). https://doi.org/10.1007/s10800-006-9127-x
195. Grgur, B.N., Žeradjanin, A., Gvozdenović, M.M., et al.: Electrochemical characteristics of rechargeable polyaniline/lead dioxide cell. J. Power Sour. **217**, 193–198 (2012). https://doi.org/10.1016/j.jpowsour.2012.06.025
196. Wills, R.G.A., Collins, J., Stratton-Campbell, D., et al.: Developments in the soluble lead-acid flow battery. J. Appl. Electrochem. **40**, 955–965 (2010). https://doi.org/10.1007/s10800-009-9815-4
197. Pletcher, D., Zhou, H.T., Kear, G., et al.: A novel flow battery: a lead-acid battery based on an electrolyte with soluble lead(II): part VI. Studies of the lead dioxide positive electrode. J. Power Sour. **180**, 630–634 (2008). https://doi.org/10.1016/j.jpowsour.2008.02.025
198. Sun, Y.Z., Guo, S.C., Wang, Y., et al.: A new lead single flow battery in a composite perchloric acid system with high specific surface capacity for large-scale energy storage. J. Solid State Electrochem. **21**, 3533–3543 (2017). https://doi.org/10.1007/s10008-017-3681-5
199. Grosvenor, V.L., Pinsky, N.: Bipolar lead-acid battery plates and method of making same. US Patent US6077623, 20 Jun 2000
200. Karami, H., Shamsipur, M., Ghasemi, S., et al.: Lead-acid bipolar battery assembled with primary chemically formed positive pasted electrode. J. Power Sour. **164**, 896–904 (2007). https://doi.org/10.1016/j.jpowsour.2006.11.034
201. Bhardwaj, R.C., Than, J.: Lead acid battery with thin metal film (TMF®) technology for high power applications. J. Power Sour. **91**, 51–61 (2000). https://doi.org/10.1016/S0378-7753(00)00486-9

Haibo Lin is now a Tang Auchin distinguished professor in College of Chemistry, Jilin University, China. He also served as the director of the School of Chemical Engineering and New Energy Materials in the Zhuhai College of Science and Technology. He obtained his B.Sc., M.Sc., and Ph.D. in physical chemistry from Jilin University in 1984, 2002, and 2005, respectively. He joined the Jinxi Chemical Research Institute as an assistant engineer, engineer, and senior engineer from 1984 to 2000. In 2000, he moved to the College of Chemistry, Jilin University as an associate professor and was promoted to a full professor in 2004. He is currently a member of the Chinese Society of the Electrochemistry (CSE) Committee, vice director of the Fine Chemical Industry Society of CIESC, and vice President of the China Supercapacitors Industry Alliance (CSCI). His main research areas are electrochemical engineering (electrode materials and electrochemical reactors), aqueous rechargeable batteries, and their key materials (additive engineering and lead-carbon batteries), electrocatalysis and electrosynthesis, environmental electrochemistry.

Xueqing Qiu is currently a professor at the Guangdong University of Technology (GDUT) and the South China University of Technology (SCUT), Guangzhou, China. He received his B.Eng. degree in chemical engineering from Tsinghua University, China, in 1987, and his Ph.D. degree in chemical engineering from the South China University of Technology, China, in 1995. He has been working in the South China University of Technology since 1990, and was promoted as a full professor in 2000. He was awarded with the China Guanghua Engineering Science and Technology Award in 2018. His main research areas are lignin chemistry, high-value-added utilization of lignin, and lignin derived functional materials.

Wenli Zhang is currently a professor at the Guangdong University of Technology (GDUT), Guangzhou, China. He received his B.E. from the College of New Energy and Environment, Jilin University, China, in 2011, and his Ph.D. degree in physical chemistry from the College of Chemistry, Jilin University, China, in 2017 under the supervision of Professor Haibo Lin. From 2017 to 2020, he carried out his post-doctoral research in Professor Husam N. Alshareef's group at the King Abdullah University of Science and Technology (KAUST), Saudi Arabia. He has published > 80 papers with an *h*-index of 30. He is the winner of the 2021 "Professor Detchko Pavlov" Young Scientist Award. Currently, his research interests focus on carbonaceous materials for electrochemical industry and electrochemical energy storage applications, such as supercapacitors, lead acid batteries, and alkali metal ion batteries.